emo-1, a *Caenorhabditis elegans* Sec61p γ Homologue, Is Required for Oocyte Development and Ovulation

Kouichi Iwasaki, James McCarter, Ross Francis, and Tim Schedl

Department of Genetics, Washington University School of Medicine, St. Louis, Missouri 63110

Abstract. *emo-1(oz1)* is a member of a class of hermaphrodite sterile mutations in *Caenorhabditis elegans* that produce endomitotic oocytes in the gonad arm. Oocytes in *emo-1(oz1)* mutants exhibit multiple defects during oogenesis. After meiotic maturation, ovulation fails, trapping oocytes in the gonad arm where they become endomitotic. *emo-1* encodes a homologue of the Sec61p γ subunit, a protein necessary for translocation of secretory and transmembrane proteins into the endoplasmic reticulum of yeast and mammalian cells. A putative *emo-1* null mutation, *oz151*, displays embryonic lethality. The *oz1* sterile mutation is a transposable element insertion into the *emo-1* 3′ untranslated region that almost completely eliminates germline mRNA accumulation. Genetic mosaic analysis using the *oz1* allele indicates that *emo-1(+)* expression in germ cells is required for fertility. The J67 monoclonal antibody, which recognizes an oocyte surface antigen (Strome, S. 1986. *In* Gametogenesis and the Early Embryo. J.G. Gall, editor. Alan R. Liss, Inc., New York. 77–95.), does not stain *oz1* oocytes, a finding consistent with defective protein transport in the mutant. We propose that the *emo-1* gene product acts in the transport of secreted and transmembrane proteins in *C. elegans* oocytes, and is necessary for both oogenesis and the coupling of ovulation with meiotic maturation.

OOGENESIS, meiotic maturation, and ovulation are critical processes that prepare the oocyte for fertilization and embryogenesis in sexually reproducing metazoans (Masui and Clark, 1979). Oogenesis requires the controlled production and storage of structural proteins, enzymes, maternal mRNAs, and determinants (Davidson, 1986; Lasko, 1992). In many species, maturation requires the regulated activation of the cdc2/Cyclin B complex (Maller et al., 1989) to allow cell cycle progression from late prophase to metaphase of meiosis I. Ovulation, the release of the oocyte from the ovary, is coordinated with maturation in species as diverse as starfish (Kanatani et al., 1969), nematodes (Ward and Carrel, 1979), insects (Doane, 1960), and mammals (Channing et al., 1978). In mammals, all three processes are regulated by gonadotropin release from the pituitary, as well as by the actions of the surrounding somatic ovarian cells. Follicle cells, for instance, appear to prevent maturation by producing high levels of cAMP delivered to the oocyte via gap junctions (Buccione et al., 1990; Wickramasinghe and Albertini, 1993). Ovarian smooth muscle cells contract to expel the oocyte at ovulation (Diaz-Infante et al., 1975).

The nematode *Caenorhabditis elegans* offers an attractive system for the study of oogenesis, maturation, and ovulation owing to its genetic accessibility and the ease with which oocytes can be monitored in real time within living animals. The *C. elegans* hermaphrodite gonad is composed of two arms, each filled with germ cells that proliferate in a distal zone and enter meiotic prophase and differentiate proximally (Hirsh et al., 1976; Kimble and Ward, 1988; Clifford et al., 1994). The proximal portion of each gonad arm is enclosed by the somatic sheath, a nonstriated myoepithelium (Strome, 1986), and terminates in the spermatheca, a bag shaped structure where fertilization occurs. The spermatheca in turn connects to the centrally located uterus and vulva. The first ~40 germ cells in each arm that enter meiotic prophase differentiate as primary spermatocytes to form ~160 sperm; all subsequent germ cells differentiate as oocytes.

Late stages of oocyte development, meiotic maturation, and ovulation occur in the proximal gonad. Progressing proximally in single file, diplotene-diakinesis stage oocytes become more fully enclosed in membrane, cell and nuclear volumes increase, and the chromosomes become increasingly condensed. The most proximal oocyte undergoes maturation, a process characterized by nuclear envelope breakdown (NEBD)[1] and the transition from diakinesis to

K. Iwasaki and J. McCarter contributed equally to this work.

Address all correspondence to Dr. Tim Schedl, Department of Genetics, Washington University School of Medicine, Box 8232, 4566 Scott Avenue, St. Louis, MO 63110. Tel.: (314) 362-6164/6162. Fax: (314) 362-7855. E-mail: ts@genetics.wustl.edu. K. Iwasaki's current address is Department of Genetics, SK-50, University of Washington, Seattle, WA 98195.

1. *Abbreviations used in this paper:* DAPI, diamidinophenylindole; Emo, endomitotic oocytes in the gonad arm; NEBD, nuclear envelope breakdown; RFLP, restriction fragment length polymorphism.

prometaphase, and is ovulated. At ovulation, increasingly frequent and intense contractions of the sheath pull the dilating distal spermatheca over the maturing proximal oocyte so that the oocyte leaves the gonad arm and enters the spermatheca (Ward and Carrel, 1979; McCarter, J., and T. Schedl, manuscript in preparation). The oocyte is fertilized immediately by activated sperm and then transferred to the uterus where it completes the divisions of meiosis I and II and begins embryogenesis.

At present, little is known concerning the regulation of oocyte meiotic maturation in *C. elegans* and how this process is coordinated with ovulation. However, previous observations (Ward and Carrel, 1979), as well as data reported here and elsewhere (McCarter, J., and T. Schedl, manuscript in preparation), indicate that oocyte meiotic maturation is coupled in time to the ovulation process. In wild-type gonads, an ~6-min interval separates the beginning of nuclear envelope breakdown at maturation and spermatheca dilation at ovulation.

Two lines of evidence indicate that failed ovulation resulting from defective sheath and/or spermathecal function leads to sterility. First, ablation of proximal sheath cells or distal spermathecal cells often disrupts ovulation with the result that oocytes undergo normal meiotic maturation but remain trapped within the gonad arm (McCarter, J., and T. Schedl, manuscript in preparation). Trapped oocytes do not remain quiescent, but instead undergo multiple rounds of endomitotic DNA replication, resulting in aberrant polyploid oocytes. We refer to endomitotic oocytes in the gonad arm as an Emo phenotype. Second, an Emo phenotype is also seen in mutants of genes likely to be required for sheath cell function or differentiation. For example, in *mup-2(e2346ts)* (Myers et al., 1996), sheath cells are incapable of contracting; oocytes mature in the gonad arm and become endomitotic without being ovulated. *mup-2* encodes a homologue of Troponin T, a known muscle contraction regulator. The Emo phenotype is also observed at low penetrance in mutants of *ceh-18*, a POU-domain homeobox transcription factor that is expressed in the sheath (Greenstein et al., 1994). A simple explanation for why unovulated oocytes become endomitotic is that this behavior represents the normal outcome for *C. elegans* oocytes that undergo meiotic maturation without subsequent fertilization. Consistent with this idea, in wild-type hermaphrodites that have exhausted their sperm supply, unfertilized oocytes undergo endomitosis after ovulation into the spermatheca and uterus (Ward and Carrel, 1979).

How are the events of meiotic maturation within the oocyte coupled to the events of sheath contraction and spermathecal dilation within the somatic gonad at ovulation? In this work, we characterize a new sterile mutant, *emo-1(oz1)*, that exhibits an Emo phenotype of endomitotic oocytes in the gonad arm. *emo-1(oz1)* was chosen for characterization because the terminal phenotype suggested that the mutation might disrupt aspects of late oocyte development, maturation, or ovulation. We used time lapse Nomarski microscopy to demonstrate that oocytes in *emo-1(oz1)* are trapped in the gonad arm by defective ovulation. However, unlike *mup-2* and *ceh-18* mutants, the initial defect in *emo-1(oz1)* occurs in the oocyte itself rather than in the surrounding somatic gonad. Cloning and sequencing of *emo-1* reveals that the gene encodes a homologue of the Sec61p γ subunit. The Sec61p complex plays a role in protein translocation into the ER in both yeast and mammalian cells (Dobberstein, 1994; Schekman, 1994). We hypothesize that signaling from the oocyte to the somatic gonad (spermatheca and/or sheath) may couple oocyte maturation with ovulation in *C. elegans*, and that defective protein translocation in *emo-1(oz1)* oocytes may interfere with such signaling and thereby disrupt ovulation. According to this hypothesis, the oocyte is an active rather than passive participant in ovulation.

Materials and Methods

General Methods and Alleles

General methods for culturing, handling, and genetic manipulation of *C. elegans* were as described (Brenner, 1974; Sulston and Hodgkin, 1988). Experiments were carried out at 20°C unless otherwise noted. This paper follows the standard *C. elegans* nomenclature (Horvitz et al., 1979). The mutations, genetic markers, deficiencies, and balancer chromosomes used were (summarized by Hodgkin et al., 1988): LGII: *mut-2(r459)* (Collins et al., 1987). LGIII: *dpy-17(e164)*, *ncl-1(e1865)*, *unc-36(e251)*. LGIV: *fem-1(hc17ts)*, *unc-24(e138)*, *fem-3(e1996)*, *him-8(e1489)*. LGV: *dpy-11(e224)*, *unc-42(e270)*, *unc-41(e268)*, *act-3(st22)*, *emo-1(oz1, oz151)*, *spe-10 (hc104ts)*, *sma-1(e30)*, *sqt-3(sc63ts)*, *sDf35*, *ctDf1*, *ctDp11*, *nT1*, *nT1n754d*, *eDf1*, *eT1*. LGX: *let-2(g30ts)*.

Mutant Isolation

emo-1(oz1) was isolated from strain TR679 (Collins et al., 1987) as a spontaneous sterile mutant in the course of isolating new *fog-2* alleles. In this screen, TR679 hermaphrodites were crossed with N2 males, and cross-progeny males were subsequently crossed to *unc-51(e369) fog-2(q71)* females. Rare female cross-progeny were recovered and outcrossed to recover new noncomplementing *fog-2* alleles. One of these animals was heterozygous for *emo-1(oz1)* and segregated homozygotes with a sterile phenotype different from the *fog-2* phenotype. *emo-1(oz1)* was placed in a wild-type N2 (Bristol variety) genetic background by repeatedly crossing heterozygotes with N2 males followed by recombining linked markers (*unc-42* and *sma-1*) on and off the *emo-1(oz1)* chromosome.

A second mutant, *emo-1(oz151)*, was isolated based on its failure to complement the hermaphrodite sterile phenotype of *emo-1(oz1)*. *unc-42(e270)* hermaphrodites were mutagenized with EMS (Brenner, 1974) and crossed with males of a wild isolate CB4855 (so-called Mr. Vigorous, Hodgkin, J., personal communication). Single F1 progeny males were mated with four *unc-42(e270) emo-1(oz1) sma-1(e30)/nT1 V*; *let-2(g30) X* adult hermaphrodites at 20°C and shifted to 25°C. The F2 generation contains only *let-2(g30)* heterozygous cross-progeny as both *let-2(g30)* homozygous self-progeny and hemizygous XO cross-progeny are inviable at 25°C. Candidates for new *emo-1* alleles were identified by screening for sterile *unc-42* cross-progeny on these plates and recovered by picking heterozygous siblings. From 8152 mutagenized haploid genomes (from the total number of successful matings), one allele (*oz151*) was recovered. To remove possible linked mutations, markers flanking *emo-1 (unc-41* and *sma-1*) were recombined onto the *oz151* chromosome.

Cytological Analysis of Germline Phenotype

Germline phenotypes were examined in live animals by Nomarski optics (Sulston and Hodgkin, 1988), and in extruded fixed gonads using epifluorescence as described (Francis et al., 1995). Dissected gonads were examined using the following reagents and fixations. To visualize DNA, gonads were fixed in 100% methanol for 5 min or in 3% formaldehyde for 2 h and stained with DAPI (diaminophenoylindole; Molecular Probes, Inc., Eugene, OR). To visualize tubulin, gonads were fixed in formaldehyde and methanol, and incubated with the mouse monoclonal N357 against β-Tubulin (Amersham Corp., Arlington Heights, IL) and a fluorescein-labeled goat anti-mouse IgG secondary (Chemicon International, Inc., Temecula, CA). The mouse monoclonal J67 (Strome, 1986; a gift from Susan Strome) and DTAF-conjugated goat anti-mouse IgG secondary (Chemicon International, Inc.) were used to detect the J67 oocyte surface antigen

after formaldehyde fixation and acetone post-fix. MEX-3, an oocyte cytoplasmic protein, was visualized with rabbit polyclonal anti–MEX-3 (Draper, B. and J. Priess, personal communication; a gift from Bruce Draper and Jim Priess) and the rhodamine-conjugated goat anti–rabbit secondary after MeOH fixation. Embryonic egg shells were detected with Calcofluor white M2R (Sigma Chemical Co., St. Louis, MO). After formaldehyde fixation, animals were incubated for 5 min in 0.2 mg/ml fresh Calcofluor in PBS. Microscopy was performed using a microscope (Axioskop; Carl Zeiss, Inc., Thornwood, NY) equipped with DIC and epifluorescence optics. Images from negatives were scanned with a scanner (ES1200C; Epson, Inc., Torrance, CA), transferred to a Power Macintosh 7100 (Apple Inc, Cupertino, CA), assembled with Photoshop 3.0 (Adobe Systems, Inc., Mountain View, CA) or Canvas 3.5 (Deneba, Inc., Miami, FL), and printed on a dye-sublimation printer (Phaser 440; Tektronix Inc., Beaverton, OR).

Time Lapse Nomarski Video Analysis

Recorded videos of oocyte development, maturation, and ovulation from wild-type (N2) and *emo-1(oz1)* animals were compared to identify any deviations from normal in *oz1*. The events occurring in wild-type oocytes are described briefly in Ward and Carrel (1979) and in this paper (see Results). A more detailed version of our observations will be published elsewhere (McCarter, J., and T. Schedl, manuscript in preparation). Worms were anesthetized for 45 min with 0.1% tricaine and 0.01% tetramisole in M9 buffer (modified from Kirby et al., 1990; Sigma Chemical Co.). Tricaine/tetramisole blocks gross movement while still allowing oocyte maturation and ovulation. Animals were viewed with a Zeiss Axioplan on a slide (with an agar pad, anesthetic solution, and the edges covered by plastic film wrap). Recordings were performed at 20–23°C. The microscope was connected to a CCD video camera module (XC-75; Sony Corp., Park Ridge, NJ) and S-VHS VCR (ag6720A; Panasonic, Secaucus, NJ). Time lapse recordings were viewed at 12× real time. Sheath activity was quantitated by visually counting the number of contractions occurring in the myoepithelium over 3-min units. Contractions were counted twice and averaged (SD of counts = 0.67 contractions/min).

Genetic Mapping, Physical Mapping, and Cloning of emo-1

emo-1(oz1) was positioned relative to genetic markers on LGV by three factor mapping (Fig. 1 *a*; Table I). To localize the gene for cloning, we narrowed the *emo-1* region by mapping within the *spe-10* and *act-1,2,3* interval and by determining the end point of the deficiency *sDf35*. *emo-1* maps to the right of *spe-10* and to the left of the *act-1,2,3* locus, which has a known physical map location. *sDf35* deletes *unc-42* and *spe-10* but not *act-1,2,3*. *unc-42 emo-1(oz1)/sDf35 trans*-heterozygotes are Unc and self-fertile indicating that *sDf35* does not delete *emo-1* (Fig. 1 *a*). The possibility that *emo-1(oz1)/deficiency* is wild type was eliminated through the isolation of *emo-1(oz151)*, a putative null allele that is homozygous lethal (see below). The right end point of *sDf35*, which served as the left boundary for *emo-1*'s initial physical map position, was identified by the STS (sequence-tagged site) PCR deletion mapping method of Barstead et al. (1991). PCR primers for cDNA clones mapping to this region (Fig. 1 *b*) were generated and used to assay whether the STSs were deleted by *sDf35*. Primers for cm04e7 produced no PCR products from *sDf35* homozygotes, but did generate a PCR product of the expected size using N2 embryos. On the other hand, primers for *ceh-22*, cm06a5, and *act-3* generated PCR products of expected sizes using both *sDf35* homozygotes and N2 embryos. PCR primers for *gld-1* (Jones and Schedl, 1995) on chromosome I were included as an internal positive control in all PCR reactions. Therefore, we conclude that the right end point of *sDf35* lies in the interval between cm04e7 and *ceh-22* (Fig. 1 *b*).

The region between the *sDf35* end point and *act-1,2,3* is spanned by 17 cosmids. Using these cosmids as probes for Southern blot hybridization, three restriction fragment length polymorphisms (RFLPs) were detected where *emo-1(oz1)* differed from N2: (*1*) a 1.6-kb insertion (RFLP 1), (*2*) a 2.3-kb insertion (RFLP 2), and (*3*) a new PstI site (RFLP 3). Recombination mapping was used to demonstrate that RFLP1 and RFLP3 are separable from *emo-1(oz1)* (Table I and Fig. 1 *b*). First, *act-3* recombinants were generated. Of six recombinants isolated between *act-3(st22)* and *emo-1(oz1)* and analyzed by Southern blot, three were found to result from recombination between *act-3* and RFLP 1, and three from recombination between RFLPs 1 and 2. No recombinants were isolated between RFLP 2 and 3. Second, of five recombinants isolated between *spe-10 (hc104)* and *emo-1(oz1)*, three were in the *spe-10*–RFLP 3 interval, and two were in the RFLP 3–RFLP 2 interval. No recombinants were isolated between RFLP 2 and 1. The data identified RFLP2 as the only candidate for an *oz1* mutation since it was the only RFLP not easily separable from *emo-1*. (RFLP 1 and 3 were renamed *ozP1* and *ozP2*, respectively.) Wild-type DNA fragments that detect RFLP 2 in Southern blot hybridization

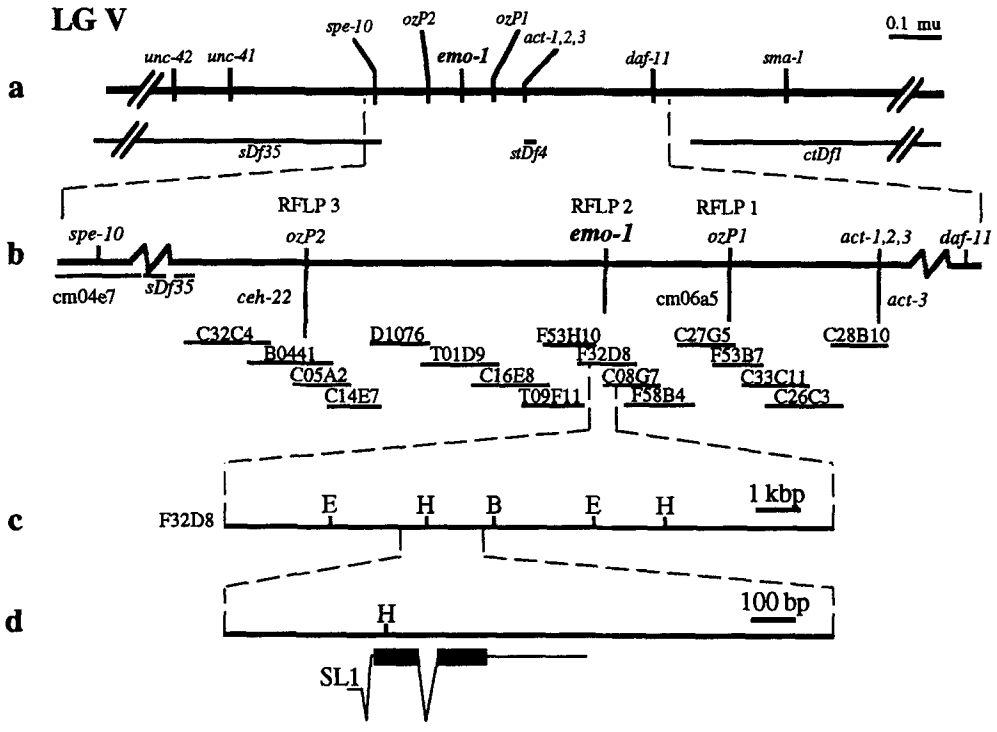

Figure 1. The genetic and physical map of the *emo-1* region on chromosome V. (*a*) genetic map. Gene positions are based on Table I except for *unc-42* and *sma-1*. The deficiencies *sDf35*, *stDf4*, and *ctDf1* are shown. End points were determined by STS–PCR mapping (see Materials and Methods). The scale of 0.1 map unit is indicated. (*b*) Physical map. The map shows genes, RFLPs, a deficiency (*sDf35*), STSs (cm04e7, *ceh-22*, cm06a5, and *act-3*), and cosmid names with relative positions. The locations of *spe-10* on the left and *daf-11* on the right are not to scale. (*c*) An enlargement of a portion of the cosmid F32D8. Restriction enzyme sites are shown as *B*, BamHI; *E*, EcoRI; *H*, HindIII. Bar indicates 1 kbp. (*d*) A further magnification of the restriction map. Coding regions, exons, and an intron of the *emo-1* gene are shown by boxes, horizontal lines, and slanted lines, respectively. The 5′ end of the *emo-1* mRNA contains an SL1 trans-splice leader sequence. Bar indicates 100 bp.

Table I. Genetic Mapping of emo-1

Parental genotype	Recombinant phenotype	Recombinant genotype	Nunber of recombinants
dpy-11 unc-42/emo-1	Dpy	*dpy-11 unc-42/dpy-11 emo-1*	22/22
	Unc	*dpy-11 unc-42/unc-42*	15/15
unc-42 sqt-3/emo-1	Sqt	*unc-42 sqt-3/emo-1 sqt-3*	5/14
		unc-42 sqt-3/sqt-3	9/14
	Unc	*unc-42 sqt-3/unc-42 emo-1*	6/12
		unc-42 sqt-3/unc-42	6/12
unc-41 sma-1/emo-1	Sma	*unc-41 sma-1/emo-1 sma-1*	7/12
		unc-41 sma-1/sma-1	5/12
	Unc	*unc-41 sma-1/unc-41 emo-1*	7/17
		unc-41 sma-1/unc-41	10/17
emo-1 sma-1/spe-10	Sma	*emo-1 sma-1/spe-10 sma-1*	11/11
		emo-1 sma-1/sma-1	0/11
unc-41 emo-1/spe-10	Unc	*unc-41 emo-1/unc-41 spe-10*	3/6
		unc-41 emo-1/unc-41	3/6
emo-1 sma-1/daf-11	Sma	*emo-1 sma-1/daf-11 sma-1*	6/14
		emo-1 sma-1/sma-1	8/14
unc-41 emo-1/daf-11	Unc	*unc-41 emo-1/unc-41 daf-11*	10/10
		unc-41 emo-1/unc-41	0/10
unc-41 emo-1/act-1	Unc	*unc-41 emo-1/unc-41 act-1*	18/18
		unc-41 emo-1/unc-41	0/18
emo-1 sma-1/act-1	Sma	*emo-1 sma-1/act-1 sma-1*	13/16
		emo-1 sma-1/sma-1	3/16
unc-42 emo-1 sma-1/act-3	Sma	*unc-42 emo-1 sma-1/act-3 sma-1*	37/47
		unc-42 emo-1 sma-1/sma-1	10/47
unc-42 emo-1 ozP1 sma-1/act-3	Sma	*unc-42 emo-1 ozP1 sma-1/ozP1 sma-1**	3/6
		*unc-42 emo-1 ozP1 sma-1/sma-1**	3/6
unc-42 ozP2 emo-1 sma-1/spe-10	Unc	*unc-42 ozP2 emo-1 sma-1/unc-42 ozP2**	2/5
		*unc-42 ozP2 emo-1 sma-1/unc-42**	3/5

*Restriction fragment length polymorphisms (*ozP1* and *ozP2* were detected by Southern hybridization (see Fig. 1) .

were cloned, sequenced, and analyzed. Sequence analysis of mutants revealed that *oz1* and *oz151* contain lesions in the only transcription unit found in the region (see Results and Fig. 5). Four independent PCR reactions from *emo-1(oz151)* all showed the same single base change from N2, thereby verifying that the detected change is not a PCR artifact.

Nucleic Acid Preparation and Analysis

Worms were grown and genomic DNA was isolated as described by Hodgkin and Sulston (1988). Genomic DNA was digested by restriction enzymes and analyzed by Southern blot hybridization using *C. elegans* cosmid DNA as probes. *Escherichia coli* strains harboring these cosmids were obtained from MRC Laboratory of Molecular Biology in England (courtesy of Alan Coulson). Cosmid DNA fragments that detected the *oz1* RFLP were cloned into pBluescript SK+ to generate pE114 1-2 (5-kb HindIII fragment) and pE129 1-5 (4-kb BamHI–EcoRI fragment) (see Fig. 1 *c*). These plasmids were used for fluorescent dye sequencing analyzed by an automated sequencer (ABI7000; Perkin-Elmer Applied Biosystems Inc., Foster City, CA). Protocols for sequencing reactions and data processing programs were provided by the *C. elegans* Genome Project Group at Washington University in St. Louis (courtesy of P. Green, L. Hillier, and R. Waterston).

Two partial *emo-1* cDNAs were obtained by a reverse PCR method using emo-1.+4Eco and emo-1.R3Bam for 5′ and 3′ RACE (Garriga et al., 1993). A filter for Northern hybridization was kindly provided by Allan Jones. *oz1* and *oz151* mutant alleles were sequenced from PCR products as described (Halloran et al., 1991). Primers used for these sequencing reactions and other PCRs were as follows: emo-1.+4Eco, GGAATTCCCAATCAATAACATCATCGTC; emo-1.+3, ATTCTTCGTCAAACTCATCC; emo-1.R4, AAACGAATGGACAAAAAAGG; emo-1.R1, ATAGTGGAGAATCCTGTCTG; emo-1.R2, ACATAGAAAAGAACAACCCG; emo-1.+1, TTGGCGATGCGTTTTTCTTTTG; emo-1.R3Bam, CGGGATCCGATGATGTTATTGATTGGG; TC4.In1, CATTTATTCTGGTCATTCCC; cm04e7a, CGATGGATGTTGGGATGTTC; cm04e7b, CGTCAGGGAAATCGGACAAG; cm06a5a, TTGGAGTTACCCCAGCATTTG; cm06a5b, TGCAGACACAGATGGAAGAAC; act-3a, GCCACATAAGAAGACCCCAC; act-3b, TTTACCAGAAAATGAGCCCG.

Construction of emo-1 Transgenic Lines

Transformation rescue (Mello et al., 1991) was performed to test whether cosmids or plasmids containing the *emo-1* sequence could rescue the *oz1* or *oz151* mutations. Rol-6 dominant marker DNA was coinjected with either a cosmid (F32D8, see Fig. 1 *b*) or plasmids (pE129 1-5 and pE114 1-2) into the following strains: N2, *unc-42 emo-1(oz1)/nT1*, or *unc-42 emo-1(oz151) sma-1/nT1*. At the concentrations of 0.1, 2, and 20 μg/ml of either cosmid or plasmid, a few F1 Rol animals were found, but none gave heritable transgenic lines. In contrast, when a control cosmid (F53B7 at 2 μg/ml) with Rol-6 plasmid or Rol-6 plasmid alone was injected into N2 or *unc-42 emo-1(oz1)/nT1* strains, many F1 Rol animals were produced and stable transgenic lines were easily established (data not shown). Injection of either F32D8 or pE129 1-5 and pE114 1-2 at very low DNA concentration (0.01 μg/ml) did result in some stable lines. However, at this concentration the molar ratios between the *emo-1* DNA and the Rol-6 plasmid were very low (1/100,000 for F32D8, and 1 / 20,000 for pE129 1-5 and pE114 1-2). It is likely that neither cosmid nor plasmid DNA were incorporated into extrachromosomal arrays. These results might reflect toxicity of *emo-1* or a linked gene at a high dose. Because of the failure to establish any stable transgenic lines, we could not test for rescue of the *oz1* and *oz151* mutations. When pE129 1-5, pE114 1-2, and *Rol-6* DNA were injected into *unc-42 emo-1(oz151) sma-1/nT1* animals, a few viable Unc Sma Rol F1 animals were found. However, these animals did not produce any progeny, and we do not know whether these animals were transiently rescued or exceptional double recombinants of the genotype *unc-42 emo-1(oz151) sma-1/unc-42 emo-1(+) sma-1* which happen to be sterile. Since transgenic expression of many germline expressed genes in *C. elegans* is problematic, these Unc Sma Rol F1 animals may have been rescued for the somatic but not the germline *oz151* phenotypes.

In Situ Hybridization of Dissected Gonads

DNA probes for *emo-1* were generated from two partial cDNAs cloned in pBluescript SK+: one (pE132) extends from the 5′ SL1 spliced leader through codon 65, and the other (pE145) extends from codon 60 through

the 3′ Poly A. Inserts of both clones were amplified by PCR using primers to the T3 and T7 vector sequences and gel purified. To generate single-stranded sense and antisense probes labeled with digoxigenin, asymmetric PCR was done as described (Patel and Goodman, 1992) using ~100 ng of purified double-stranded insert and an oligonucleotide primer to either T3 or T7 promoter sequences. PCR products were ethanol precipitated, resuspended in 300 μl hybridization buffer (HB) (Patel and Goodman, 1992), and diluted 1:3 in HB just before use.

For in situ hybridizations, gonads were dissected from wild-type and *emo-1(oz1)* animals as described (Francis et al., 1995), and fixed for 2 h in 3% formaldehyde; 0.25% glutaraldehyde; 0.9 M Na_2HPO_4 (pH 7.2). All subsequent manipulations were done by suspending the dissections in PBS containing 0.1% Tween 20 (PBTw) and using low speed centrifugation (setting 2 of a table-top clinical centrifuge) to pellet gonads with attached carcasses. Briefly, dissections were processed as follows: (*a*) wash 1× in 4 ml PBTw; (*b*) postfix 5 min in cold (−20°C) 100% methanol; (*c*) wash 3× in PBTw; (*d*) digest 30 min in 3 ml 20–40 μg/ml protease K in PBTw; (*e*) wash 3× in PBTw; (*f*) fix 15 min in 3% formaldehyde; 0.25% glutaraldehyde; 0.9 M Na_2HPO_4 (pH 7.2); (*g*) wash 3× in PBTw; (*h*) incubate 15 min in PBTw; 2 mg/ml glycine; (*i*) wash 3× in PBTw. For subsequent steps, the dissections were transferred to 6 mm (ID) by 50-mm (length) glass culture tubes and processed as follows: (*a*) wash 1× in PBTw; (*b*) incubate 10 min in 1 part PBTw; 1 part HB at 48°C; (*c*) prehybridize 1 h in 400 μl HB; (*d*) hybridize 36 h in 100 μl HB containing digoxigenin-labeled probe; (*e*) wash 3 × 5 min at 48°C in HB; (*f*) wash 4 × 30 min at 48°C in HB; (*g*) wash 1× at 48°C in 1 part HB/1 part PBTw; (*h*) wash 2× at 48°C and 2× at room temperature in PBTw. Probes were visualized by incubating in alkaline phosphatase–conjugated antidigoxigenin (Boehringer Mannheim Biochemicals, Indianapolis, IN) overnight at 4°C and developing alkaline-phosphatase activity for 2–4 h as described (Seydoux and Fire, 1994). Samples were then placed in PBTw/100 ng/ml DAPI and mounted on a 2% agarose pad for viewing with a B-MAX 60F microscope (Olympus Corp. Precision Instruments Division, Lake Success, NY) equipped with a video CCD camera (470-DEI-T; Optronics Engineering, Goleta, CA). Images were collected using the application NIH image 1.58 (Wayne Rasband, NIH), and assembled in Adobe Photoshop 3.0. Antisense probes specific for the 5′ and 3′ halves of *emo-1* mRNA gave identical results and were used together to obtain the data in Fig. 8. Single-stranded sense DNA probes processed in parallel gave no signal after 4 h of color development. As a positive control to demonstrate probe accessibility, we have found that mRNAs for *gld-1* and *mes-6* can be detected in all regions of the adult hermaphrodite germ line. Therefore, inaccessibility is unlikely to account for our failure to detect *emo-1* mRNA in the distal mitotic region of the wild-type germ line.

Mosaic Analysis

The strain used for mosaic analysis [*dpy-17(e164) ncl-1(e1865) unc-36(e251); unc-42(e270) emo-1(oz1); ctDp11*] was constructed as follows. *dpy-17 ncl-1 unc-36; him-8(e1489); her-1(y101hv1) unc-42; ctDp11* males (Hunter and Wood, 1992) were mated with *unc-42 emo-1/nT1* hermaphrodites. Non-Unc progeny were individually cloned and their genotype confirmed as *dpy-17 ncl-1 unc-36/+; him-8/+;* + unc-42 emo-1/*her-1 unc-42* +; *ctDp11*. Among progeny, non-Unc animals were cloned and their genotypes deduced. Animals that produced Dpy Unc Ste progeny at high frequencies were picked and their genotypes confirmed.

Mosaic animals were identified by directly screening L3 larva or young adults with Nomarski (DIC) optics for a mosaic pattern of the Ncl phenotype. Cells used for deducing mosaicism (see Fig. 9 legend) were identified by morphology and position as described (Sulston and Horvitz, 1977; Sulston and White, 1980; Sulston et al., 1983). Brood sizes of these mosaic animals were determined by counting the number of progeny including dead eggs. The germline phenotype at the adult stage was examined using Nomarski optics.

Results

emo-1(oz1) Mutant Oocytes Undergo Endomitotic DNA Replication in the Gonad Arm

emo-1(oz1) was isolated as a hermaphrodite sterile mutant from a genetic background [TR679 *mut-2(r459)*] where transposable elements are actively mobile (Collins et al., 1987). The *emo-1(oz1)* phenotype is fully penetrant. Sterility is associated with oocytes in the proximal gonad arm that contain polyploid nuclei. Because polyploid nuclei arise from endomitotic replication of the DNA within the oocyte (see below), the gene has been named *emo-1*. The Emo designation is used for the phenotype of endomitotic oocytes in the gonad arm and is distinct from the phenotype of endomitotic oocytes in the uterus seen when fertilization fails (Ward and Carrel, 1979; see Discussion). *emo-1(oz1)* was chosen for further characterization because the terminal phenotype of endomitotic oocytes in the gonad arm suggested that the mutation might disrupt aspects of late oocyte development, maturation, or ovulation.

We compared germline morphology in *emo-1(oz1)* and wild type by Nomarski DIC microscopy and by DAPI epifluorescence staining for detection of DNA. By Nomarski, the nucleus of each oocyte in the wild-type hermaphrodite gonad stands out against the more refractile cytoplasm with a clearly defined spherical boundary (Fig. 2 *a*). In contrast,

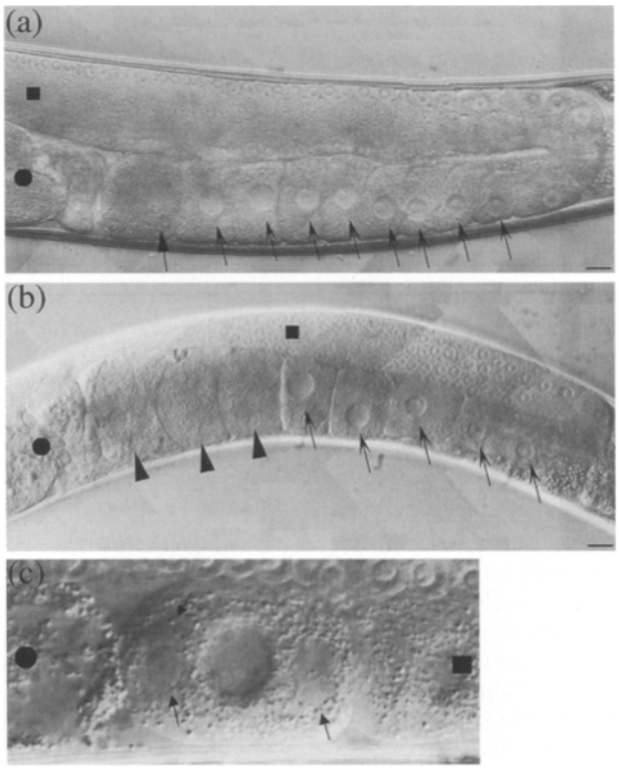

Figure 2. Nomarski (DIC) micrographs of wild-type and *emo-1(oz1)* gonads. (*a*) N2 wild-type gonad. Nuclei in diakinesis stage oocytes (*open arrows*) of the proximal arm display intact nuclear envelopes. The maturing first oocyte (*filled arrow*) is beginning nuclear envelope breakdown and cortical rearrangement. (*b*) *emo-1(oz1)* gonad. Nuclei in diakinesis stage oocytes (*open arrows*) of the midproximal arm display intact nuclear envelopes. Proximal endomitotic oocytes (*arrowheads*) lack clearly delineated nuclei. Nuclei can appear disorganized, lobed, or enlarged. Nuclei are often not visible because cycles of nuclear envelope breakdown and reformation occur during the endomitotic process (see Results). (*c*) An *emo-1(oz1)* oocyte before endomitosis. Cytoplasmic deposits (*arrow*) and rounding of the oocyte are typical abnormalities observed during late oogenesis before endomitosis in *emo-1(oz1)* hermaphrodites. Distal and proximal orientation are indicated by a square and circle, respectively. Bar, 10 μm.

the nuclei of proximal oocytes in *emo-1(oz1)* homozygous adult hermaphrodites are often indistinct from the surrounding cytoplasm, enlarged relative to wild type, or nonspherical (Fig. 2 *b*). By DAPI, gonads dissected from wild-type hermaphrodites have proximal oocytes with condensed chromosomes in diakinesis (Fig. 3 *a*). In contrast, each proximal oocyte in *emo-1(oz1)* hermaphrodites is filled with a polyploid blob (*arrowheads*). However, many aspects of *emo-1(oz1)* germline development are normal. For instance, *oz1* hermaphrodites exhibit no abnormalities in germline development as L4s and young adults. Proliferation in the distal gonad, entry and progression through meiotic prophase, and sperm formation appear normal. All the somatic gonad cells are present and display their normal morphology. *oz1* males are morphologically normal and partially fertile in mating tests, suggesting that *oz1* sperm are functional (Table II). Providing *oz1* hermaphrodites with wild-type sperm by mating with wild-type males does not restore fertility.

Three observations reveal that the polyploid genome of the *oz1* oocytes arises by ongoing endomitotic cycling. First, by time lapse video Nomarski microscopy, cycles of nuclear envelope breakdown and reformation are observed. Second, endomitotic oocytes can be observed with either condensed or decondensed chromosomes (Fig. 3 *c*). When chromosomes are condensed, a large number of chromosomes (>50) can be observed. Third, the proximal oocytes, which become endomitotic before more distal oocytes, show more intense DAPI staining, suggesting that additional rounds of DNA replication have occurred. The absence of karyokinesis and cytokinesis in endomitotic *oz1* oocytes likely reflects the lack of centrioles in unfertilized oocytes (see Discussion).

emo-1(oz151) Homozygotes Are Embryonic Lethal

To determine the range of phenotypes which result from mutations in *emo-1*, we performed a noncomplementation screen to recover new alleles (see Materials and Methods). A screen of 8,152 mutagenized haploid genomes resulted in the isolation of *emo-1(oz151)*, a likely null mutant as judged by molecular criteria (see below). *oz1/oz151* hermaphrodites are viable and show an Emo phenotype similar to that seen in *oz1* homozygotes (Table II). However, unlike *oz1* homozygotes, sperm appear swollen in *oz1/oz151* hermaphrodites and males (Table II). *oz1/oz151* males also display variable defects in tail morphology. Most *emo-1(oz151)* homozygous embryos contain approximately the normal number of cells, but arrest before morphogenesis (Table II).

emo-1(oz1) Oocytes Are Defective in Development and Ovulation

To determine the origin of the endomitotic phenotype in *emo-1(oz1)* homozygotes, we directly observed defects which occur in *oz1* oocytes during development, maturation, and ovulation by time lapse video Nomarski microscopy (Ward and Carrel, 1979; McCarter, J., and T. Schedl, manuscript in preparation) in anesthetized animals (Kirby et al., 1990). Measurable characteristics of oocytes were compared between wild type (N2) and *oz1* (Table III). The terminal phenotype of endomitotic oocytes in the gonad arm in *oz1* could arise from a number of possible causes. Hypotheses considered include: (*a*) defective ovulation causes a normally maturing oocyte to become trapped in the gonad arm; (*b*) sperm, inappropriately activated in the gonad arm, stimulate the oocyte to exit meiotic prophase prematurely; or (*c*) an oocyte defective in meiotic cell cycle regulation exits diakinesis of meiotic prophase prematurely.

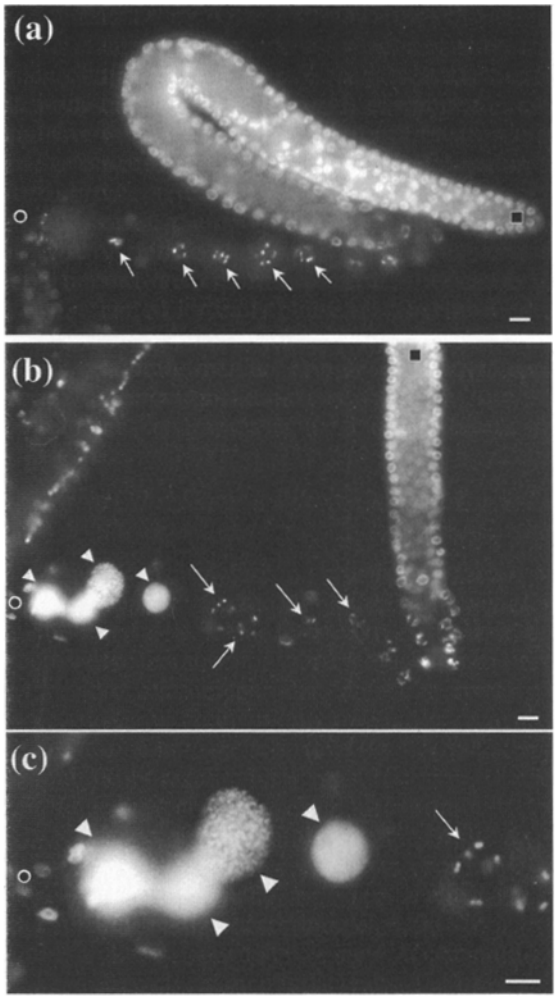

Figure 3. Fluorescence micrographs of wild-type and *emo-1(oz1)* dissected gonads stained with DAPI for DNA. (*a*) N2 wild-type gonad. Chromosomes of oocytes in the proximal gonad arm are condensed in diakinesis (*open arrows*). The most proximal oocyte appears to be maturing with the chromosomes in prometaphase. (*b*) *emo-1(oz1)* gonad. Chromosomes of oocytes in the midproximal gonad arm are condensed in diakinesis (*open arrows*). Proximal endomitotic oocytes are polyploid with large accumulations of DNA (*arrowheads*). (*c*) *emo-1(oz1)* endomitotic oocytes. Right arrowhead indicates an endomitotic nucleus in interphase with decondensed chromosomes. Left arrowhead indicates an endomitotic nucleus with condensed chromosomes. *Square*, distal gonad; *Circle*, proximal gonad. Bar, 10 μm.

Wild-type Oocyte Development, Maturation, and Ovulation. In the *C. elegans* hermaphrodite, oocytes are ovulated in an assembly-line fashion at ~50-min intervals. As developing oocytes reach diakinesis stage of meiotic prophase I in the proximal gonad arm, chromosomes become increasingly condensed, while the nuclear envelope

Table II. Terminal Phenotypes of emo-1 Homozygotes and trans-Heterozygotes

Genotype	*ozl/ozl**	*ozl/ozl51*‡	*ozl51/ozl51*§
Phenotype	endomitotic oocytes in the gonad arm (Emo)‖	Emo, some swollen sperm¶	embryonic lethal**

* *unc-42(e270) emo-1(ozl).*

‡ *unc-42(e270) emo-1(ozl)/unc-42(e270) emo-1(ozl51).*

§ *unc-42(e270) emo-1(ozl51), unc-42(e270) emo-1(ozl51) sma-1(e30),* or *unc-41(e268) emo-1(ozl51) sma-1(e30)*

‖ Three out of 108 animals produced 1 to 2 progeny before becoming *Emo.* These progeny grew normally and became *Emo* as adults. Males of *him-8(e1489); emo-1(ozl)* have normal germline morphology and 50% of them (n = 44) produced cross progeny. We have not determined whether the inefficient production of cross progeny is due to a sperm defect or a subtle defect in male mating behavior or function.

¶ Morphology of some sperm is normal, but some sperm are swollen. This abnormal sperm phenotype is not observed in *ozl* homozygote. We have not tested *ozl/ozl51* males for fertility.

** Most *ozl51* homozygotes undergo embryonic proliferation producing approximately the wild-type number of cells during embryonic proliferation, but arrest without undergoing morphogenesis and elongation (94.4%, n = 161). Some arrest earlier in embryogenesis with fewer cells (4.3%), or at a later stage with some pharyngeal formation and hypodermal elongation (1.2%). Cell number in *ozl51* homozygotes = 605 ± 72 (n = 10), determined by counts of DAPI stained nuclei. Wild-type embryogenesis produces approximately 560 surviving cells and approximately 110 cell deaths (Sulston et al., 1983).

remains intact. During late oocyte development, nuclear volume increases, the nucleolus disappears, and the nucleus migrates to the distal surface of the oocyte. The oocyte in the most proximal position undergoes maturation, the process of exit from diakinesis of meiotic prophase. Maturation includes nuclear envelope breakdown (NEBD) and oocyte cortical rearrangement where the oocyte changes from a cylindrical to ovoid shape. Meanwhile, contractions of the somatic sheath increase in rate and intensity. Ovulation occurs ~6 min after the beginning of maturation; the distal spermatheca dilates and is pulled over the first oocyte by the contracting sheath.

ozl Oocyte Development. Many aspects of oocyte development appear normal in *ozl*, including the time of nucleolus reabsorption and nuclear migration, as well as oocyte and nuclear size (Table III legend). However, several abnormalities become evident during *ozl* oogenesis well before the oocyte matures and becomes endomitotic (Table III). (*a*) In wild type, no oocyte cytoplasmic movement occurs before ovulation, whereas in *ozl*, oocyte cytoplasmic granules show directed streaming during oogenesis. (*b*) In wild type, the oocyte cytoplasm is uniform by Nomarski microscopy, whereas in *ozl*, large refractile bodies appear transiently in the oocyte cytoplasm (Fig. 2 *c*). (*c*) In wild type, the nucleus is centered equidistant from the oocyte's dorsal and ventral surfaces (Fig. 2 *a*), whereas in *ozl*, the oocyte nucleus often drifts to the dorsal or ventral surface (Fig. 2 *b*). (*d*) In wild type, the oocyte appears rectangular in cross-section until maturation (Fig. 2 *a*), whereas in *ozl*, oocytes can have a more rounded appearance (Fig. 2 *c*). These findings reveal that *emo-1(ozl)* oocytes are abnormal before becoming endomitotic.

ozl Oocyte Maturation. Oocyte maturation in *ozl* is similar to maturation in wild type. In wild type, oocyte maturation, including NEBD, always occurs in the most proximal oocyte positioned next to the spermatheca. In *ozl*, NEBD always occurs in the oocyte next to the spermatheca, or in the most proximal oocyte which is not already endomitotic. Therefore, even though oocytes are trapped in the gonad arm in *ozl*, a temporal progression of meiotic maturation is maintained; oocytes that mature early (more proximal) become endomitotic before those that mature later (more distal). Also, as in wild type, NEBD in *ozl* always occurs in an individual oocyte after the events of oocyte development are complete. The interval between successive maturations is slow in *ozl* (81 min ± 27, n = 4) relative to wild type (54 min ± 12, n = 11). These findings are not supportive of the hypothesis that premature exit from meiotic prophase is the cause of endomitosis in *ozl* oocytes (hypothesis c); if oocytes were exiting prophase prematurely, NEBD might occur out of proximal-distal order and during the events of oocyte development. Further, a shorter interval between subsequent NEBD's relative to wild type might be expected if oocytes were prematurely exiting prophase.

ozl Oocyte Ovulation. Ovulation in *emo-1(ozl)* hermaphrodites shows abnormalities in both spermatheca and sheath behavior when compared with wild type (Table III). In 4 of 11 attempted ovulations in *ozl*, the spermatheca failed to dilate and the oocyte remained in the gonad arm. In 6 of 11 ovulations, the oocyte left the gonad, but the ovulation was abnormal with respect to spermathecal dilation and/or the sheath contraction profile (Table III). After the first failed ovulation, all oocytes behind the first are trapped. As a result, most gonad arms expel only a few oocytes before becoming plugged. The *ozl* oocytes that are ovulated become endomitotic in the uterus. Based on Nomarski appearance and Calcofluor staining, no egg shell is formed (data not shown). Since *ozl* sperm are functional and wild-type sperm do not restore fertility (see above), the postovulation defects appear to be oocyte specific.

In summary, time lapse video Nomarski microscopy supports the hypothesis that *ozl* oocytes become endomitotic in the gonad arm following failed ovulation rather than following premature exit from meiotic prophase. Further, several oocyte abnormalities are evident during oogenesis before maturation and attempted ovulation.

Feminization Delays Ovulation and the Onset of Endomitosis in emo-1(ozl)

As a further test of the idea that the *ozl* Emo phenotype is a result of an ovulation defect, we took advantage of the effect of germline feminization on maturation and ovulation. *C. elegans* females, generated using mutations that disrupt germline sex determination, lack sperm (see legend Fig. 4). In virgin females, oocytes maintain an extended cell cycle arrest in diakinesis of meiotic prophase after the events of oocyte development. However, maturation and ovulation do occur stochastically at approximately 1/10th the frequency observed when sperm are present (McCarter, J., and T. Schedl, manuscript in preparation). The first maturation and ovulation is delayed by ~3 h in females relative to hermaphrodites. This delay is particularly striking since females actually produce their first oocytes several hours earlier than hermaphrodites (because no sperm are made first) (Kimble et al., 1984). We reasoned that if endomitotic oocytes arise in the gonad arm in *emo-1(ozl)* after failed ovulation, then the onset of the endomitotic phenotype should be delayed in *ozl* females relative to *ozl* hermaphrodites.

*Table III. Abnormal Aspects of Development and Ovulation in emo-1(oz1) Oocytes**

Phenotypes‡	Wild type proportion of animals displaying phenotype	*emo-1(oz1)* proportion of animals displaying phenotype
Oocyte development		
Cytoplasmic transient refractile bodies	0/15	16/29
Cytoplasmic streaming	0/15	12/27
Rounded edges§	0/15	12/27
Nucleus at dorsal or ventral surface‖	0/15	8/17
Oocyte ovulation¶		
Ovulation fails (oocyte remains in arm)	0/15	4/11
Ovulation abnormal but succeeds (oocyte leaves arm)	1/10	6/11
Spermatheca dilation abnormal**	0/15	6/11
No dilation	0	4
Late dilation	0	1
Incomplete dilation (oocyte pinched into 2 pieces)	0	1
Sheath contractile activity abnormal‡‡	1/10	9/11
No peak of activity	0	1
Early peak	1	3
Late peak	0	2
High peak	0	5
Low peak	0	1

*Oocyte development, maturation, and ovulation were examined by time-lapse video Nomarski DIC microscopy in anesthetized animals. Visible abnormalities listed in the table were also observed in nonanesthetized animals.

‡Over 30 phenotypes (i.e., visible morphologies, measurable distances, timed events) were compared between wild-type hermaphrodites and *emo-1(oz1)*. The following phenotypes were similar in wild-type and *emo-1(oz1)* oocytes: time of nucleolus disappearance, completion of nuclear migration to the distal surface of the oocyte and time of the migration, distance of the nucleus to the distal surface of the oocyte before and after migration, nuclear diameter, length and width of the oocyte, time of NEBD, time of cortical rearrangement, time of nuclear disappearance after NEBD, time of uterine entry after successful ovulations. Additional data not shown.

§Wild-type developing oocytes are cylindrical cells which become ovoid at maturation (cortical rearrangement). In *oz1*, developing oocytes often have somewhat rounded edges, but are not ovoid like mature oocytes.

‖The oocyte nucleus is usually centered in wild-type oocytes and off center in *emo-1(oz1)*. Nuclei <1.5μm from the dorsal or ventral surface are scored as being at the surface.

¶Only oocytes that reach the most proximal position in the gonad arm and have the opportunity to be ovulated are considered in this section of the table. Abnormalities include defects in either spermathecal dilation or the profile of sheath contractile activity. One the most proximal oocyte fails to be ovulated and becomes endomitotic in a gonad arm, additional oocytes behind it mature and become endomitotic in a proximal to distal progression ($n = 4$).

** In wild type, the spermatheca dilataes for ovulation approximately 6 min after NEBD. Dilation is wide enough for the distal spermatheca to move over the proximal oocyte. In all four *oz1* cases where no dilation occurred, the oocyte remained in the gonad arm. The late dilation observed occurred >19 min after NEBD.

‡‡In wild type, sheath contractile activity increases in the 50 min before ovulation from 5 to 15 contractions per min. The peak rate ranged from 12 to 17. In all cases but one, the peak of contractile activity corresponded with the time of ovulation. Contractile activity falls rapidly after ovulation. In *oz1*, contractile activity sometimes peaked 3 min before or 3 min after ovulation. Peaks from 18 to 23 contractions per min were seen, as well as one peak below 11. Two additional abnormalities in *oz1* are not listed in the table: in one case, sheath contractions did not fall below 10 contractions per min after ovulation (wild-type range = 2–7). In another case, sheath activity did not recover after falling. The subtotals sum to >9 because some ovulations showed multiple abnormalities.

We found that endomitotic oocytes form in *emo-1(oz1)* females, but that the onset of endomitosis is delayed. This was true for both *unc-24(e138) fem-3(e1996); emo-1(oz1)* females, and *fem-1(hc17ts); emo-1(oz1)* females. Time course experiments were performed on synchronous populations of worms to compare the time of onset of endomitosis in *oz1* hermaphrodites with *oz1* females (Fig. 4; see Materials and Methods). In multiple trials, feminization always caused a delay of several hours in the time of onset of *oz1* endomitosis. This behavior is consistent with a defect in ovulation (hypothesis a).

The existence of endomitotic oocytes in virgin *emo-1(oz1)* females also demonstrates that *oz1* endomitosis is not sperm dependent and so eliminates the hypothesis that inappropriately activated sperm trigger oocytes to become endomitotic (hypothesis b). Further, the observed delay in the onset of endomitosis in *oz1* females is not predicted by the hypothesis that oocytes become endomitotic due to premature exit from meiotic prophase (hypothesis c). Premature exit from prophase during oocyte development would not be delayed by feminization since the diakinesis arrest in females occurs after oocyte development; feminization might even hasten the onset of endomitosis since oocytes are produced earlier in females. However, it remains a formal possibility that feminization might delay a premature exit from meiotic prophase if there is an interval between the female diakinesis arrest point and the normal maturation point, and the *emo-1(oz1)* defect causes exit in this interval. In summary, our results in *emo-1(oz1)* females provide support for the hypothesis of defective ovulation, and allow us to dismiss the possibility of sperm-triggered endomitosis. The results discount but do not eliminate the possibility that the *emo-1(oz1)* oocyte prematurely exits diakinesis.

Do Meiotic Divisions Occur Before Endomitosis in emo-1(oz1) Oocytes?

In wild-type oocytes, maturation and fertilization is followed by the divisions of meiosis I and II during which the oocyte pronucleus uses a meiosis-specific, barrel-shaped spindle (Albertson, 1984). We were unable to detect meiotic divisions in *emo-1(oz1)* oocytes by two procedures. First, gonads from adult *fem-1; emo-1(oz1)* worms where endomitosis was just beginning were dissected and stained with DAPI and an anti-tubulin monoclonal antibody (Francis et al., 1995). (The *fem-1* mutation was included to eliminate sperm and spermatocytes which might be confused with polar bodies.) No meiotic spindles, mitotic spindles, or obvious reorganization of tubulin was detected in

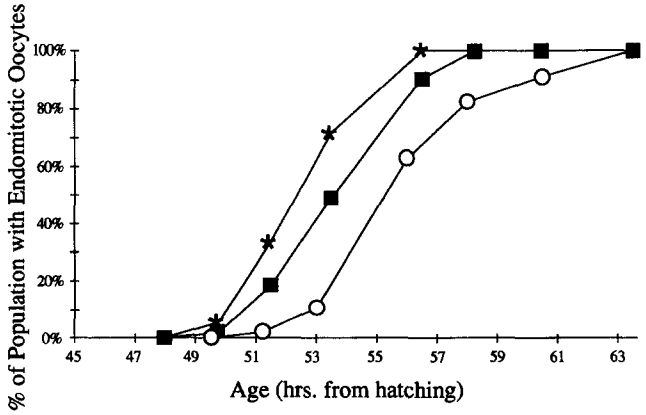

Figure 4. Representative time course showing the onset of the endomitotic phenotype in populations of *emo-1(oz1)* hermaphrodites and females. [*unc-24(e138)*; *emo-1(oz1)* vs. *unc-24(e138) fem-3(e1996)*; *emo-1(oz1)*] (*C. elegans* can be transformed from a hermaphrodite to a female using one of several mutations that effect germline sex determination. In *fem-1,-2*, or *-3* or *fog-1*, *-2*, or *-3*, germ cells that would normally form sperm differentiate as oocytes [for review see Clifford et. al., 1994]). Black stars indicate percent of *oz1* hermaphrodites with endomitotic oocytes in either the uterus or gonad arm. Black squares indicate percent of *oz1* hermaphrodites with endomitotic oocytes in the gonad arm. (Endomitotic oocytes appear in the uterus first because *oz1* hermaphrodites usually ovulate a few oocytes successfully. These oocytes are not fertilized and become endomitotic in the uterus.) White circles indicate percent of *oz1* females with endomitotic oocytes in the gonad arm. Oocytes are not observed in the uterus of *oz1* females. Similar results were obtained in three trials; at the 50% point, the delay between endomitosis appearing in the *oz1* hermaphrodite gonad arm and *oz1* female gonad arm was 2.0 ± 0.6 h. Average population size per trial: 46 hermaphrodites and 46 females.

oz1 oocytes (n = 546), nor were polar bodies observed. Second, oocyte maturation was observed under Nomarski optics in *oz1* animals. After nuclear envelope breakdown and reformation, animals were fixed and DAPI stained for DNA; no polar bodies were visible (n = 2). Therefore, it is possible that *emo-1(oz1)* oocytes begin endomitotic cycling without having executed one or both meiotic divisions.

emo-1 Encodes a Homologue of the Sec61p γ Subunit

The *emo-1* gene was molecularly defined by positional cloning (see Materials and Methods). *emo-1(oz1)* was mapped to LGV between *spe-10* and the actin cluster by three-factor mapping (Table I, Fig. 1 *a*). The boundaries of the *emo-1* physical map position were defined as the right breakpoint of the deficiency *sDf35* and the *act-1,2,3* locus (Fig.1 *b*). Of three tightly linked RFLP's found in the *oz1* mutant but absent from N2, recombinational segregation revealed that only RFLP 2 is consistent with a lesion in *emo-1* (Table I, see Materials and Methods). DNA fragments that detected RFLP 2 in Southern blot hybridization were cloned and sequenced. The GENE FINDER program (Green and Hillier, personal communication) predicted a gene of two exons (Fig. 5 *a*) encoding a putative protein of 68 amino acids.

By sequence analysis, the *oz1* allele was found to contain an insertion of the transposable element Tc4 (Yuan et al., 1991; Li and Shaw, 1993) in the 3′ untranslated region (UTR) of the putative *emo-1* gene (Fig. 5, *a* and *b*). To confirm that the cloned gene was *emo-1*, a DNA fragment from *emo-1(oz151)* was amplified by PCR and sequenced. *emo-1(oz151)* is a G-to-A change at the putative initiation methionine codon (ATG) of the cloned gene (Fig. 5 *a*). Since use of the next Met codon for translation would result in a protein that has only the COOH-terminal 31 amino acids, *emo-1(oz151)* is likely to be a null allele. No deficiencies exist which delete *emo-1*, so we are unable to test whether the *oz151* mutation behaves as a genetic null.

Based upon the predicted sequence of *emo-1*, PCR primers for the open reading frames were generated. The 5′ and 3′ RACE-PCR products were cloned and sequenced. The 5′ UTR is 8-nt long and linked to an SL1 leader sequence (Fig. 1 *d* and Fig. 5 *a*). The 3′ UTR is 220 nt long and is followed by a poly(A) tail (Fig. 5 *a*).

The putative EMO-1 protein is highly homologous to yeast SSS1 (40% identical) and the Sec61p γ subunits from canine (82%), human (85%), and rice (68%) (Fig. 6). Sec61p γ, which is predicted to have one membrane spanning domain (Hartmann et al., 1994), is a part of Sec61p, a protein complex responsible for translocation of secretory and transmembrane proteins into the ER (Schekman, 1994; Dobberstein, 1994).

emo-1 mRNA Is Expressed in the Germ Line

Northern analysis, using an *emo-1* cDNA probe, revealed

Figure 5. Sequence of the *emo-1* gene. (*a*) The *emo-1* genomic sequence is shown with proposed amino acids of the encoded protein. Nucleotide and amino acid positions are indicated by the numbers to the right of each sequence line. The first methionine codon begins at nucleotide 49 of the genomic sequence shown. Splice sites are indicated by arrowheads (*black arrowhead*, a 5′ splice site; *white arrowheads*, 3′ splice sites). The poly(A) site is indicated by a dot at nucleotide 520. Positions of mutations found are shown with boxes along with allele numbers. The *oz151* allele is a point mutation, G to A. The *oz1* allele is a Tc4 insertion in the 3′ UTR. (*b*) Junction sequences of the *oz1* allele. A Tc4-transposable element is inserted into nucleotide 324, creating a three-base duplication (*boxed*). The Tc4 sequences are underlined. These sequence data are available from GenBank/EMBL/DDBJ under accession number U53785.

a band of ~0.7 kb that is present in both total *C. elegans* RNA and a poly A fraction (Fig. 7). This size is consistent with our cDNA analysis which predicts a transcribed sequence of 450 nt and a poly A tail of 100–200 nt. To determine whether *emo-1* is restricted to the germ line, RNA was analyzed from sterile *glp-4(bn2)* hermaphrodites that lack almost all germ cells at the restrictive temperature (Beanan and Strome, 1992). We find that *emo-1* mRNA accumulates to a high level in *glp-4(bn2)* animals, indicating that *emo-1* is expressed in at least some somatic tissues.

Expression of *emo-1* at the single cell level was examined by in situ hybridization using a single-stranded DNA probe. In both wild-type hermaphrodite (Fig. 8 *a*) and male (Fig. 8 *b*) germ lines, we detect no *emo-1* mRNA in proliferating cells of the distal mitotic region, but do see strong signal that begins at the approximate position where germ cells switch to a meiotic cell cycle. In the hermaphrodite, presumptive female germ cells maintain *emo-1* mRNA accumulation as they progress through the stages of meiotic prophase and form oocytes. In contrast, *emo-1* mRNA levels in the adult male germ line, though high at early stages of meiotic prophase, drop to an undetectable level by the late pachytene stage. No signal is seen in spermatocytes or spermatids in males or in hermaphrodites. Based on these results, we conclude *emo-1* is expressed in the germ line, but that *emo-1* mRNA accumulation is apparently regulated in a sex- and stage-specific manner.

Examination of dissected preparations indicates that *emo-1* expression is not ubiquitous in somatic tissues. Among somatic tissues of the hermaphrodite that are extruded after dissection, we find strong staining of the intestine and weak staining of the spermatheca. To examine the somatic sheath cells in a situation where germline signal was not a factor, we viewed the sheath cells surrounding unstained sperm in the proximal germline of young adult hermaphrodites. No accumulation of *emo-1* mRNA was observed in this situation (data not shown), indicating that

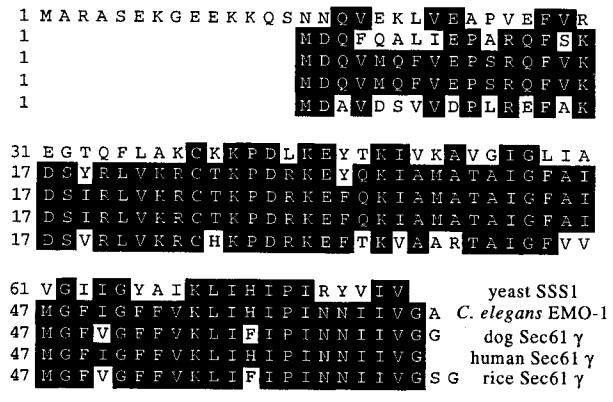

Figure 6. Comparison of the putative *C. elegans* EMO-1 protein and the Sec61p γ subunit from other species: yeast (*Saccharomyces cerevisiae*), dog (*Canis familiaris*), human (*Homo sapiens*), and rice. The sizes of these proteins are 81 amino acids (yeast), 68 (*emo-1*), 68 (dog), 67 (human), and 69 (rice). Amino acid positions are indicated by the numbers to the left of each protein. Black boxes indicate amino acids conserved in the majority of the sequences shown. Identities of these proteins to EMO-1 are 40% (yeast SSS1), 82% (dog Sec61p γ subunit), 85% (human Sec61p γ subunit), and 68% (rice).

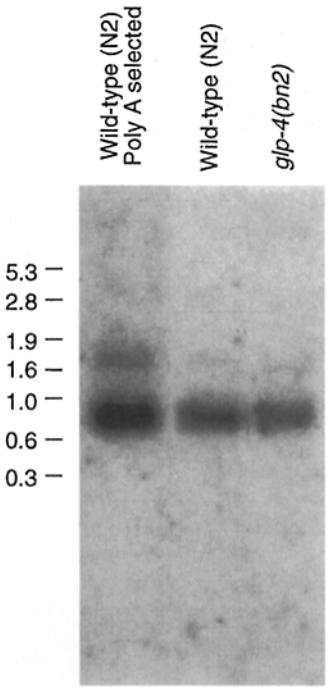

Figure 7. Northern hybridization of *emo-1* mRNA. Lanes include Poly(A) RNA and total RNA from the *C. elegans* wild-type strain N2 and total RNA from *glp-4(bn2)*. A strong band was visible at 0.7 kb in all lanes. A weak band was also observed at 1.7 kb and has not been characterized further. RNA marker sizes are shown at the left side of the panel. *glp-4(bn2)* has a greatly reduced germ line at the restrictive temperature (Beanan and Strome, 1992). Actin RNA is detectable across lanes at comparable levels (data not shown). Germline-specific RNA (*gld-1*) was not detected in the *glp-4* lane (data not shown).

emo-1 is not expressed by the somatic sheath. In wild-type males, we find *emo-1* expression in the somatic gonad (seminal vesicle and/or vas deferens) and the intestine. Unexpectedly, however, male intestines consistently show much weaker signal than hermaphrodite intestines, suggesting that *emo-1* expression in the intestine may be under sex-specific regulation (Shen and Hodgkin, 1988).

In situ analysis of hermaphrodite *emo-1(oz1)* germ lines indicates that the allele *oz1*, which contains a Tc4 element insertion in the gene's 3′ UTR, is associated with a diminished level of *emo-1* RNA accumulation in the germ line. Most individual *emo-1(oz1) XX* germ lines have no detectable signal while others show greatly diminished signal (<10% of wild type) (Fig. 8 *c*). Interestingly, although diakinesis-stage oocytes never show strong signal, oocytes that have begun endomitosis sometimes display nuclear staining (Fig. 8, *d* and *e*). Cytoplasmic accumulation of *emo-1(oz1)* transcripts in the hermaphrodite intestine is also diminished and much of intestinal signal appears to be nuclear. Despite this effect on *emo-1* expression, *emo-1(oz1)* hermaphrodites have yolk droplets in the pseudocoelom, which suggests the mutant intestine may retain functions required for yolk protein secretion. Why we detect nuclear signal in *emo-1(oz1)* intestinal cells and endomitotic oocytes, but not in female germ cells in meiotic prophase (pachytene through diakinesis) is not clear, but may reflect a greater instability of nuclear *emo-1(oz1)* transcripts in germ cells progressing through meiotic prophase. Nonetheless, these data suggest that the primary effect of the *oz1* Tc4 insertion on germline expression of *emo-1* involves reduced transcript accumulation, rather than reduced translational efficiency.

Emo Sterile Phenotype in emo-1(oz1) Results from a Defect within the Oocyte

By time lapse microscopy, *emo-1(oz1)* has defects in both oocyte development and the functions of the somatic

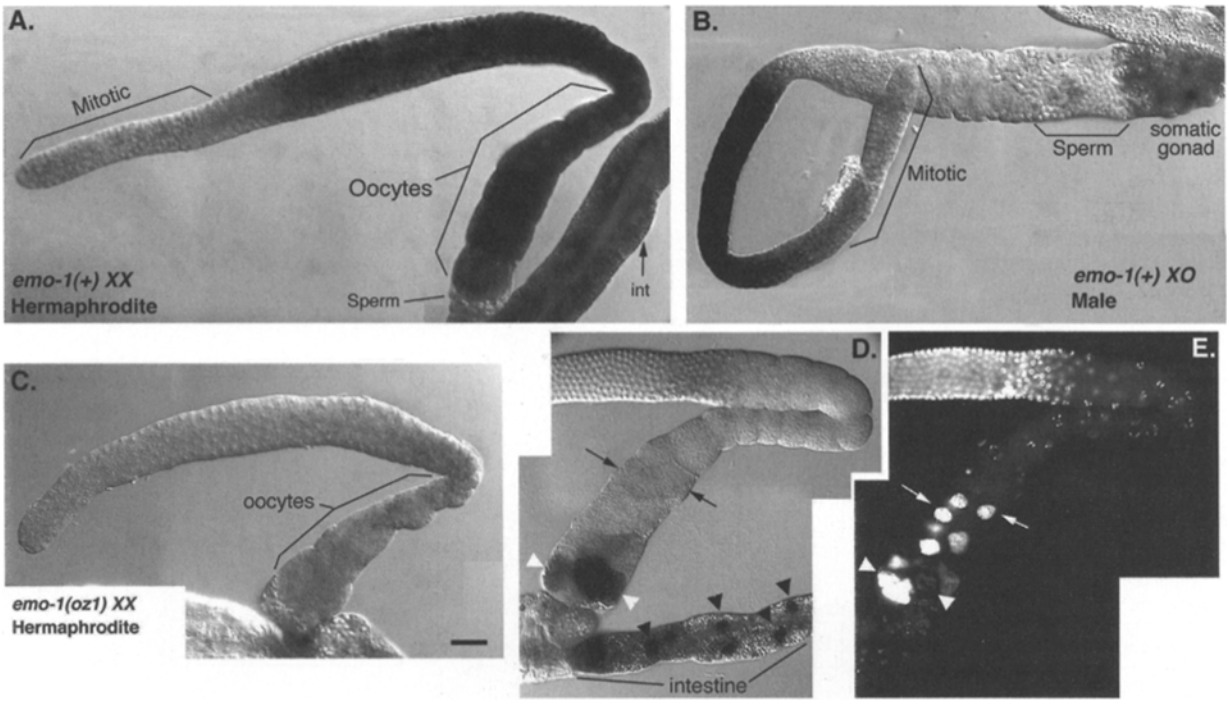

Figure 8. Detection of *emo-1* transcripts by in situ hybridization. Dissected gonads hybridized with a single-stranded anti-sense *emo-1* DNA probe are shown visualized with Nomarski optics (*A–D*) or with epifluorescence to show DAPI staining of DNA (*E*). In both wild-type *XX* hermaphrodite (*A*) and *XO* male (*B*) gonads, pachytene-stage germ cells show strong signal while distal mitotic cells show little or no signal. Female *XX* germ cells maintain *emo-1* RNA accumulation as they form oocytes, whereas male *XO* cells lose *emo-1* transcript. Stronger *emo-1* signal is seen in the hermaphrodite intestine (*int*) than in the male intestine. Somatic gonad signal in *XO* males appears localized to seminal vesicle and vas deferens cells. (*C–E*) *XX emo-1(oz1)* hermaphrodites showing signal only slightly above background in diakinesis-stage oocytes and undifferentiated germ cells. The young adult gonad (*C*) contains no endomitotic oocytes, whereas the slightly older gonad (*D* and *E*) contains many endomitotic oocytes (*arrows*), some of which (*white arrowheads*) show *emo-1* signal. *emo-1* signal in *emo-1(oz1)* intestines is predominately nuclear (*black arrowheads*).

sheath and spermatheca during ovulation. Hypothetically, *emo-1(+)* activity may be required in either the germ line, the soma, or both tissues for either oocyte development or ovulation. To determine conclusively where wild-type *emo-1* is needed to prevent the *oz1* Emo sterile phenotype, we performed mosaic analysis with the strain *ncl-1 unc-36; dpy-11 unc-42 emo-1(oz1); ctDp11* (see Materials and Methods). The free duplication, *ctDp11* (Hunter and Wood, 1992), contains the wild-type allele of *emo-1* and each of the markers. The Ncl-1 phenotype was used to determine which cells had lost *ctDp11* since *ncl-1* is a cell-autonomous marker (Hedgecock and Herman, 1995).

The germ line derives exclusively from the P4 cell, whereas the somatic gonad arises from within the MS lineage (Fig. 9 *a*). Loss of *ctDp11* at any point in the P lineage (P1, P2, or P4) results in sterility with the *oz1* Emo phenotype (Fig. 9, *c–e*). (Note that the losses in P4 are inferred since the Ncl-1 phenotype cannot be scored in the germ line.) When *ctDp11* is lost in the EMS or MS lineage (Fig. 9 *g*), or various other somatic lineages (Fig. 9, *f* and *h*), fertility is maintained. Since *oz1* is not a null allele, we are unable to determine whether the *emo-1* gene is still functional in the soma in an *oz1* background, or whether the gene is nonfunctional and not necessary in the soma.

From the mosaic analysis, we conclude that *emo-1(+)* is required in the germ line to prevent the *oz1* endomitotic sterile phenotype, while the presence of *emo-1(+)* in the somatic gonad is not sufficient to prevent sterility. *emo-1(oz1)* therefore differs from the two previously characterized mutants with the Emo phenotype, *mup-2(e2346ts)* and *ceh-18(mg57)*, in which sterility likely results from a primary defect in the somatic sheath (Myers et al., 1996; Greenstein, et al., 1994).

emo-1(oz1) Oocytes Fail to Express an Oocyte Surface Antigen

As a Sec61p γ homologue, the EMO-1 protein is likely to function in the translocation of secreted and cell-surface proteins into the ER. To test whether *emo-1(oz1)* oocytes are defective in such translocation, we examined *oz1* oocytes for the presence of J67, an antigen that localizes to the surface of wild-type oocytes (Strome, 1986). In wild-type hermaphrodites, the J67 monoclonal antibody stains both within the oocyte and along the oocyte surface. In females, or in hermaphrodites that have exhausted their sperm supply, diakinesis stage oocytes accumulate in the gonad and J67 staining localizes to the oocyte's surface (Fig. 10 *a*). In *oz1* hermaphrodites and females, J67 staining is absent from all oocytes in diakinesis as well as all those which have become endomitotic (Fig. 10, *b* and *c*); only background staining, similar to that seen with the secondary antibody alone, is observed. This absence of J67 staining provides evidence that *emo-1 (oz1)* oocytes are defective in protein translocation.

We also examined *emo-1(oz1)* oocytes for the presence

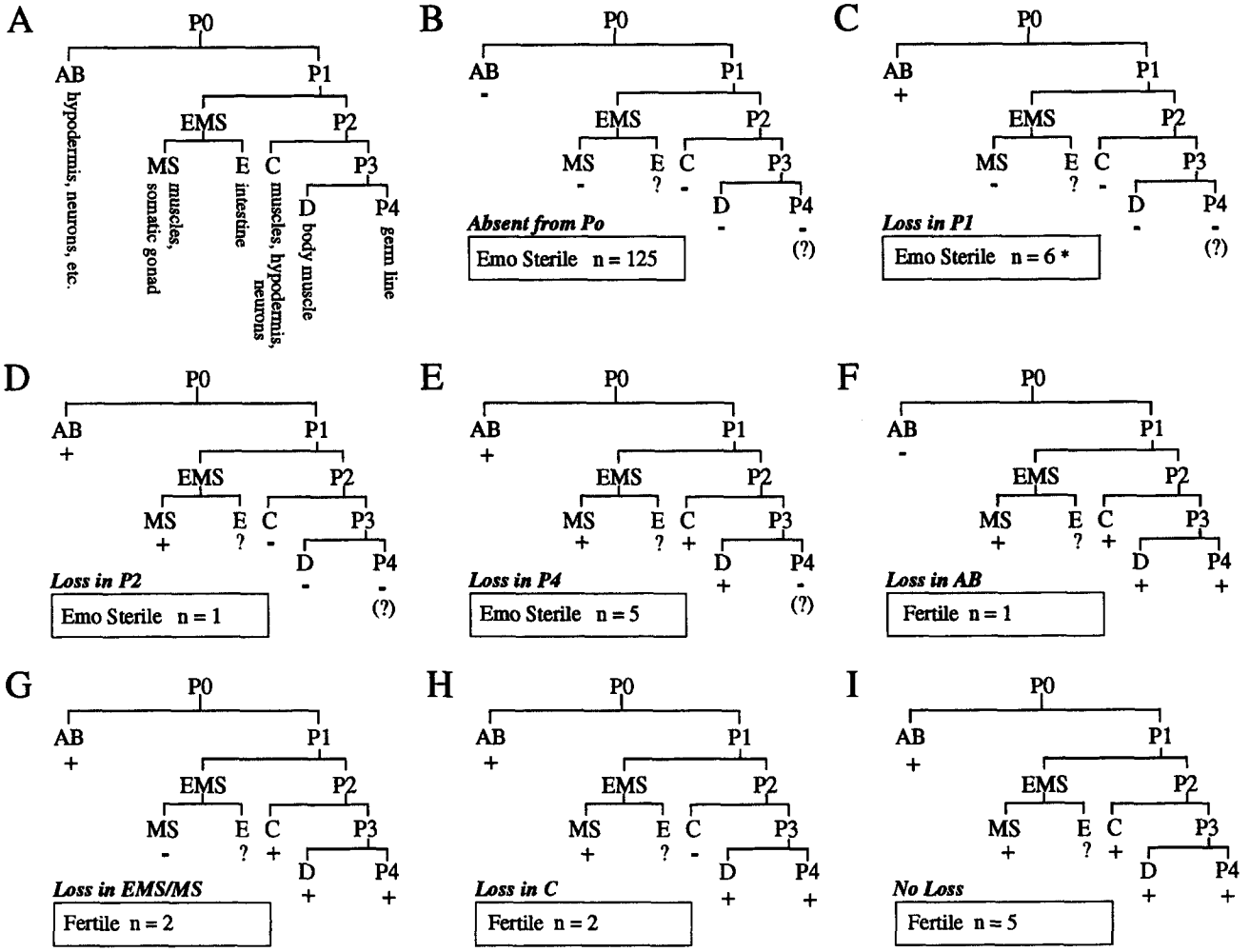

Figure 9. Mosaic analysis of the *emo-1* gene in *oz1* homozygotes. (*A*) Cell lineage of early nematode development. *P0*; the fertilized zygote, *AB* and *P1*; daughters of the fertilized zygote. Subsequent cell lineage from P1 is shown. All lineages after AB, MS, E, C, D, and P4 are omitted. The tissues generated from each blast cell are shown below. (*B–I*) Different classes of mosaic animals. The Ncl phenotype was used to deduce the point of a free duplication (*ctDp11*) loss. The Ncl phenotype is not scorable in descendants of E (the intestine) or P4 (germline) and thus its presence or absence is inferred. Points of *ctDp11* loss were determined by examining all or some of the following cells for the Ncl phenotype: the AB lineage by ASK, ADL, ASI, BUD, ALM, CAN, V5, B, ventral cord neurons, and the excretory cell, the P1 lineage by pharyngeal and body wall muscle cells and DVC, the MS/E lineage by pharyngeal and body wall muscle cells, and the C lineage by DVC and body wall muscle cells. The AB loss was initially identified by the Unc-36 phenotype. The P0 loss was determined by the Dpy and Unc phenotype and "No Loss" by the non-Dpy and non-Unc phenotype. Average brood size was determined for nonsterile animals. For AB loss (*F*), brood = 168. For E/MS loss (*G*), brood >100. For C loss (*H*), brood = 143. For no loss (*I*), brood = 162. * 1 of the 6 P1 losses did produce 18 progeny before becoming sterile.

of an oocyte cytoplasmic antigen, MEX-3. MEX-3 is a maternally provided putative RNA binding protein necessary for embryonic development (Draper, B. and J. Priess, personal communication). Antibodies directed against MEX-3 show diffuse staining in the cytoplasm of diakinesis-stage oocytes (Draper, B. and J. Priess, personal communication). In *emo-1(oz1)* hermaphrodites, MEX-3 is present in the cytoplasm of diakinesis-stage oocytes, but is often found in aggregates (data not shown). Aggregated MEX-3 may mark the same oocyte cytoplasmic abnormalities seen as transient refractile bodies by Nomarski microscopy. MEX-3 staining disappears in oocytes when they become endomitotic. The finding of abnormal staining patterns in *emo-1(oz1)* during oocyte development with both J67 and MEX-3 antibodies supports the conclusion from time lapse video that *oz1* oocytes are abnormal before becoming endomitotic.

Discussion

We have performed a genetic, molecular, and cellular analysis of *emo-1*, a *C. elegans* gene encoding a Sec61p γ homologue. Sec61p γ proteins play an important role in the translocation of secretory and transmembrane proteins into the ER. A putative null allele, *emo-1(oz151)*, is embryonic lethal, whereas *emo-1(oz1)* is a sterile allele in which a transposon insertion into the 3′ UTR disrupts mRNA accumulation in the germline. Germline expression of *emo-1(+)* appears to be necessary and sufficient to prevent sterility. *emo-1(oz1)* is a member of a class of ster-

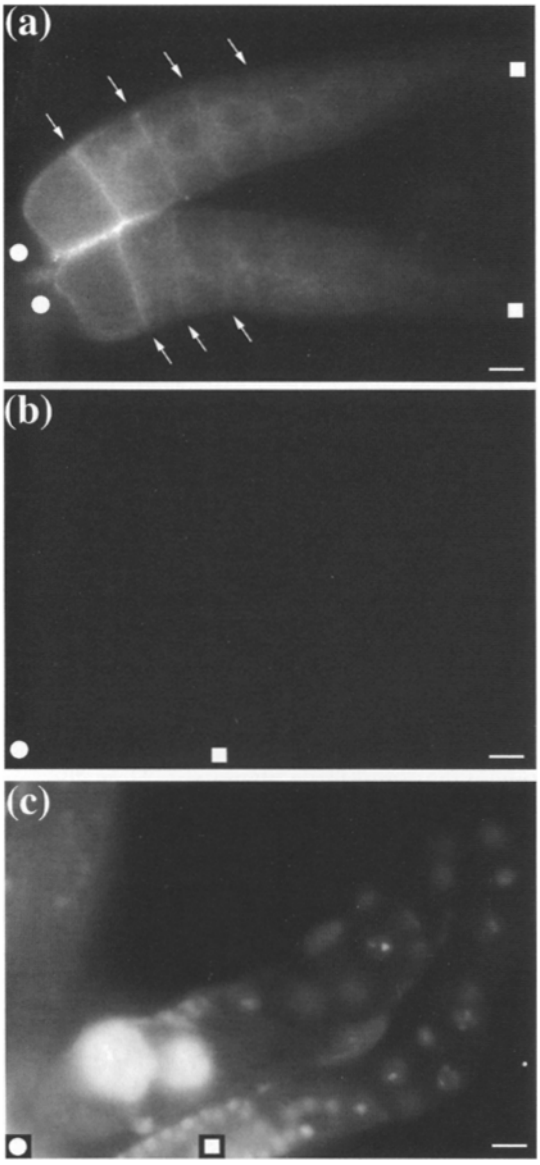

Figure 10. Fluorescence micrographs of J67 antibody (Strome, 1986) stained *fem-3(e1996)* female and *emo-1(oz1)* hermaphrodite dissected gonads. (*a*) J67 monoclonal antibody epifluorescence of *fem-3(e1996)* female proximal gonads. Arrows indicate oocyte surface reactivity to the J67 antigen. Staining internal to the oocyte is also visible. J67 antigen also appears in wild-type hermaphrodites, but surface staining is not apparent until all of the self-sperm is exhausted (data not shown). (*b* and *c*) J67 (*b*) and DAPI (*c*) epifluorescence of an *emo-1(oz1)* hermaphrodite proximal gonad. No J67 antigen is detectable on the surface or internally in either the diakinesis stage or endomitotic *oz1* oocytes. J67 antigen is also not detected in *fem-3(e1996); emo-1(oz1)* females (data not shown). *Square*, distal gonad; *Circle*, proximal gonad. The identity of the J67 antigen is unknown. Bar, 10 μm.

ile mutants in *C. elegans* that have endomitotic oocytes in the gonad arm. Our evidence suggests that *emo-1(oz1)* oocytes develop abnormally, fail to complete normal ovulation, and become trapped in the gonad arm where they become endomitotic. We propose that *oz1* oocytes may be deficient in signaling to the surrounding somatic gonad to properly modulate the spermathecal dilation and/or sheath contractions necessary for the oocyte to exit the gonad at ovulation (see below).

emo-1 Encodes a Sec61p γ Subunit Homologue

emo-1 encodes a *C. elegans* homologue of the Sec61p γ subunit (85% identical to the human Sec61p γ). The Sec61 complex is implicated in the translocation of proteins into the ER. Proteins containing signal sequences are targeted to the ER as the first step toward processing for secretion or residence in the cell membrane. The *Saccharomyces cerevisiae* SEC61 gene, which encodes Sec61p α, was defined by mutations in the gene which block the translocation of secreted products into the ER (Deshaies and Schekman, 1987). Sec61p α has multiple transmembrane domains spanning the ER (Stirling et al., 1992), and biochemical evidence supports a role in translocation (Deshaies et al., 1991; Müsch et al., 1992; Sanders et al., 1992). The Sec61p γ subunit in yeast was identified as SSS1, a high copy suppressor of SEC61 (Esnault et al., 1993), and was shown to associate with Sec61p α (Esnault et al., 1994; Panzner et al., 1995). Disruption of yeast SSS1 results in lethality and accumulation of secretory proteins in the cytoplasm. Biochemical cross-linking and reconstitution studies identified the complex of Sec61p α (Görlich et al., 1992), Sec61p β, and Sec61p γ (Görlich and Rapoport, 1993; Hartmann et al., 1994) in mammals. Further, the *E. coli* translocation proteins Sec Y, G, and E share homology to Sec61p α, β, and γ, respectively (Hartman et al., 1994). The Sec61 proteins, therefore, likely make up an evolutionarily conserved complex required for protein translocation across membranes (for review see Schekman, 1994; Dobberstein, 1994). Sec61p α appears to form a transmembrane pore that directly contacts the translocating nascent peptide chain, while Sec61p β and γ act as accessory proteins that modulate the process.

emo-1 May Act in ER Protein Translocation

Based on the homology, it is likely that *emo-1* is involved in an ER protein translocation process in the nematode. The embryonic lethal phenotype of the putative null *oz151* is consistent with a function for *emo-1* in a vital cellular process. Since *oz1* mutant hermaphrodites display defects in oogenesis, we assayed for the presence of an oocyte surface antigen recognized by the J67 monoclonal antibody (Strome, 1986). We found that the J67 antigen was absent from *oz1* oocytes (both membrane and cytoplasm) before the initiation of endomitosis, a finding consistent with oocytes being defective in ER translocation. However, the result with J67 differs somewhat from that seen for secretory proteins in the yeast mutant SSS1 where blocked translocation leads to the cytoplasmic deposition of the proteins (Esnault et al., 1993). Defective translocation in *oz1* may eliminate the J67 antigen because: (*a*) translation of the protein that J67 recognizes cannot be completed without translocation into the ER; (*b*) the protein has transmembrane domains that are unstable cytoplasmically; or (*c*) the J67 antibody recognizes a carbohydrate side-chain that is added after ER translocation. Other interpretations unrelated to translocation are also possible.

Abnormalities in the cytoplasm of *emo-1(oz1)* oocytes include refractile bodies under Nomarski optics. The ori-

gin of these cytoplasmic "deposits" is unknown. Given the role of Sec 61 in translocation, it is possible that the deposits contain untranslocated proteins, including proteins which would normally contribute to the egg shell. Additionally, sperm in *ozl/ozl51* hermaphrodites appear swollen; a defect that might also involve blocked translocation. Protein secretion (Link et al., 1992), as well as egg shell protein production (Wharton, 1983), are largely unstudied topics in nematodes. The finding of *C. elegans* mutations affecting the Sec61 complex in oocytes *(ozl/ozl)*, sperm *(ozl/ozl51)*, and embryos *(ozl51/ozl51)* thus provides an opportunity for molecular genetic studies of protein translocation in a multicellular organism, and possibly for the specific study of nematode egg shell secretion.

emo-1(ozl) Defect Is Specific to Oocytes

The *emo-1(ozl)* mutation, an insertion of the transposon Tc4 into the 3′ UTR of *emo-1*, represents a case where a lesion in a gene involved in a fundamental cellular process, ER translocation, disrupts only a single cell type, the developing oocyte. Unlike the candidate null allele, *emo-1(ozl51)*, which results in embryonic lethality, *emo-1(ozl)* confers no obvious phenotype other than hermaphrodite sterility. *ozl* mosaic animals are fertile unless the wild-type copy of the gene is lost in the germ line. The apparent specificity of *ozl* may be attributable to a combination of factors, including genetic redundancy and the mutation having a more severe effect on *emo-1* expression in the oocyte than in other cells. Consistent with the idea of genetic redundancy, not all cell types that are accessible to in situ hybridization in dissected preparations showed *emo-1* transcript accumulation. Expression was observed in several somatic tissues (intestine, spermatheca, male somatic gonad), but not in proliferating germ cells or in sheath cells of the somatic gonad. The latter cell types perhaps express another Sec61 γ subunit encoded by a different gene. However, it also appears that *ozl* affects germline *emo-1* expression more severely than it does somatic expression. Whereas *emo-1(ozl)* eliminates germline accumulation of *emo-1* mRNA, transcript accumulation in the intestine remains strong, although only a fraction of transcript is cytoplasmic. The remainder appears nuclear, arguing that the *ozl* Tc4 lesion disrupts the nuclear export/stability of *emo-1* transcript. Meiotic prophase germ line nuclei fail to show nuclear accumulation of *emo-1(ozl)* RNA, a finding that could reflect greater instability of the mutant RNAs in developing female germ cells. The greater germline transcript instability may, in large part, account for the oogenesis-limited *emo-1(ozl)* phenotype.

emo-1(ozl) Oocytes Are Defective in Ovulation

In wild-type *C. elegans* hermaphrodites, appropriate regulation of meiotic progression, maturation, ovulation, and fertilization appears to prevent oocytes from becoming endomitotic. Each oocyte in the proximal gonad arm is in diakinesis of first meiotic prophase until maturation; after maturation, the oocyte is immediately ovulated and fertilized. Observations of *emo-1(ozl)* support the hypothesis that failed ovulation results in endomitotic oocytes in the gonad arm (the Emo phenotype). First, in time lapse Nomarski videos of *ozl*, the proximal oocyte is observed to become endomitotic after ovulation fails. Both defective spermathecal dilation and abnormal sheath contraction patterns are observed. Second, in *C. elegans* females, oocytes arrest in diakinesis after the events of oocyte development and before maturation. Just as the onset of maturation and ovulation is delayed in females relative to wild-type hermaphrodites, feminization of *ozl* delays the onset of the endomitotic phenotype, a result consistent with defective ovulation. The alternative hypothesis, that activated sperm in *emo-1(ozl)* cause oocytes to become endomitotic, is eliminated by the finding of endomitotic oocytes in *emo-1(ozl)* virgin females. Another alternative hypothesis, that *emo-1(ozl)* oocytes prematurely exit diakinesis to become endomitotic, is not supported by our observations, although it cannot be eliminated (see Results).

Failed Secretion from Oocytes Is a Likely Cause for Defective Ovulation in emo-1(ozl)

Mosaic analysis, in situ hybridization, time lapse microscopy, and antibody staining patterns all reveal that the initial defect in *emo-1(ozl)* occurs in the oocyte. Yet, time lapse microscopy and feminization time course experiments indicate that defective spermatheca dilation and sheath contractile patterns during ovulation are the eventual failings that trap *emo-1(ozl)* oocytes in the gonad arm, resulting in the Emo sterile phenotype. How does an initial defect in the oocyte result in defective ovulation? The homology of the putative EMO-1 protein to Sec61p γ, and the failed presentation of the J67 oocyte surface antigen suggest that *emo-1(ozl)* oocytes may be defective in protein translocation. We hypothesize that signaling from the oocyte to the soma (spermatheca and/or sheath) through a secreted factor(s) may couple oocyte maturation and ovulation in *C. elegans*, and that defective protein translocation in *emo-1(ozl)* oocytes disrupts the signaling process.

The maturing oocyte may use secreted protein products or transmembrane proteins to modulate either dilation of the distal spermatheca and/or the frequency and intensity of contractions in the sheath. Defective signaling from the maturating oocyte in *emo-1(ozl)* might result in the spermatheca failing to dilate or sheath contractile activity failing to peak. Such direct germline regulation of activity in the surrounding soma may be necessary since neither the gonadal sheath nor spermatheca receive any input from the nervous system in *C. elegans* (White et al., 1986). While defects are observed in both the spermatheca and sheath during ovulation in *emo-1(ozl)*, it is unclear which cell type is signaled by the oocyte. For instance, it is possible that the delayed and abnormally high peak of sheath activity we occasionally observed during *ozl* ovulation was a secondary consequence of the spermatheca not dilating.

emo Mutants May Define Genes that Function in the Oocyte and Somatic Gonad for Ovulation

Directly after maturation, the oocyte is ovulated by vigorous contractions of the sheath and dilation of the spermatheca. Ovulation requires both germline and somatic gonad function; sterile mutants with the Emo phenotype

have now been found which interrupt ovulation by effecting the oocyte (*emo-1(oz1)*, this work) and the sheath (*mup-2(e2346ts)*, Myers et al., 1996, and *ceh-18(mg57)*, Greenstein et al., 1994). Ablations of sheath and spermathecal cells also disrupt ovulation (McCarter, J., and T. Schedl, manuscript in preparation). *emo* mutants arise at high frequency in general screens for steriles and alleles defining multiple loci have been isolated (our unpublished results). Some of the *emo* mutants yet to be characterized may identify genes encoding proteins which act in a pathway for germline modulation of somatic gonad activity at ovulation.

Endomitotic Replication as the Default State for Mature Unfertilized Oocytes in C. elegans

Endomitotic replication occurs in mature unfertilized oocytes in the gonad arm of *emo* mutants and in the uterus of animals where mature oocytes are ovulated without fertilization. These cases include *fer* and *spe* mutants, where sperm are incapable of fertilization (Ward and Miwa, 1978; L'Hernault et al., 1988), wild-type worms that have exhausted their sperm supply (Ward and Carrel, 1979), and female worms where occasional ovulations occur without sperm (McCarter, J., and T. Schedl, manuscript in preparation). Despite the different locations, the underlying endomitotic phenomenon may be similar: oocytes mature but are not fertilized; mitotic cycles occur with rounds of DNA replication and nuclear envelope breakdown/reformation; karyokinesis and cytokinesis do not occur. Exemplifying the similarity, when ovulation does expel an *emo-1(oz1)* oocyte from the gonad arm, it becomes endomitotic in the uterus; if not for the ovulation defect, *emo-1(oz1)* might have a terminal phenotype essentially identical to a *fer* mutant. Fertilization may fail in these cases because *oz1* oocytes cannot translocate transmembrane proteins necessary for fertilization.

Endomitotic replication appears to be a consequence of oocytes maturing without subsequent fertilization. Mature *C. elegans* oocytes contain maternally contributed messages (Kreutzer et al., 1995; Seydoux and Fire, 1994), likely including those needed for zygotic cell cycling. In wild-type animals, oocytes mature (exiting diakinesis of prophase I), are ovulated, rapidly fertilized, complete the divisions of meiosis I and II, and begin embryogenesis. Meiotic divisions use a specialized meiotic spindle made in the oocyte, while mitotic divisions require a mitotic centriole supplied by the sperm (Albertson, 1984). Endomitotic oocytes may also progress through meiosis and into mitotic cycles like those in embryos, but lacking mitotic centrioles, the cycles occur without karyokinesis or cytokinesis. It is also possible that endomitotic oocytes begin endomitotic cycles without properly completing meiosis. We never observed meiotic spindles in *emo-1(oz1)* endomitotic oocytes, although apparently meiosis I occurs in *fer-1* oocytes (Ward and Miwa, 1978). If endomitotic oocytes do begin DNA replication without completing meiosis I and II, this suggests that fertilization is required to promote meiosis I and II, and to suppress DNA replication, either directly or indirectly, during this period. Additional observations will be necessary to conclusively establish whether or not meiotic divisions occur in endomitotic oocytes.

Once endomitosis begins in *C. elegans* oocytes, cycles continue through multiple rounds so that the cell becomes polyploid. G1 and G2 cell cycle checkpoints, which prevent rounds of DNA synthesis without karyokinesis and cytokinesis in many cell types (Hartwell and Weinert, 1989), therefore seem to be lacking. This may indicate that the wild-type cycles of early *C. elegans* embryogenesis also lack G1 and G2 checkpoints, as has been found for early embryogenesis in many species (O'Farrell et al., 1989). While G1 and G2 checkpoints may not be necessary to insure S-phase/M-phase alternation for normal early embryogenesis, after the failure of fertilization and mitotic spindle introduction, the absence of checkpoints allows endomitotic cycling to occur.

Interestingly, a phenotype similar to the endomitotic oocytes seen in the gonad arm or uterus of *C. elegans* mutants is observed in the eggs of certain *Drosophila* mutants. In *Drosophila*, there is an arrest point after meiosis II, which is not present in *C. elegans*, that prevents cell cycling in wild-type unfertilized eggs (Doane, 1960; Mahowald et al., 1983). Thus, defective ovulation or fertilization in *Drosophila* would not be expected to produce endomitotic oocytes like the *emo*, *spe*, and *fer* mutants in *C. elegans*. However, mutations in *plutonium (plu)*, *gnu*, and *pan gu (png)* (Freeman et al., 1986; Freeman and Glover, 1987; Shamanski and Orr-Weaver, 1991) are defective in the postmeiosis arrest and immediately begin DNA replication (S-phase) with or without fertilization. Rounds of DNA replication occur without nuclear division and result in giant polyploid nuclei in the eggs. Cycles do not require karyokinesis. Therefore, while the initial defects in the *C. elegans* and *Drosophila* mutants described are different, in all cases, unregulated rounds of DNA replication result. These analogous terminal phenotypes may reflect a similar lack of G1 and G2 regulation of early embryonic mitotic cell cycles in both *C. elegans* and *Drosophila* embryos.

We thank Yueping Zhang, Thanh Dang, and Bart Bartlett for excellent technical assistance, Allan Jones for providing a Northern filter and discussions on molecular studies, Alan Coulson for the cosmids, Barbara Robertson and William Wood for the *ctDp11* strain, Pete Okkema and Andy Fire for *ceh-22* PCR primers, Susan Strome and Bruce Draper for antibodies, Robert Waterston for suggesting a sequencing approach for *emo-1*, members of the Schedl and Waterston laboratories for helpful discussions, and Dave Reiner, Ben Williams, Bob Clifford, and Bart Bartlett for helpful comments on this manuscript. We also thank Beth Bucher, David Greenstein, Mai Thao Le, and Carol Myers for helpful discussions regarding the Emo phenotype.

This research was supported by U.S. Public Health Service grant HD-25614 to T. Schedl. K. Iwasaki was supported by the W.M. Keck Foundation. Some of strains used in this research were provided from the *Caenorhabditis* Genetics Center at the University of Minnesota, which is supported by the National Institutes of Health National Center for Research Resources.

Received for publication 10 April 1996 and in revised form 24 May 1996.

References

Albertson, D.G. 1984. Formation of the first cleavage spindle in nematode embryos. *Dev. Biol.* 101:61–72.

Barstead, R.J., L. Kleiman, and R.H. Waterston. 1991. Cloning, sequencing, and mapping of an alpha-actinin gene from the nematode *Caenorhabditis elegans*. *Cell Motil. Cytoskel.* 20:69–78.

Beanan, M.J., and S. Strome. 1992. Characterization of a germ-line prolifera-

tion mutation in *Caenorhabditis elegans*. *Development (Camb.)*. 116:755–766.
Brenner, S. 1974. The genetics of *Caenorhabditis elegans*. *Genetics*. 77:71–94.
Buccione, R., A.C. Schroeder, and J.J. Eppig. 1990. Interactions between somatic cells and germ cells through mammalian oogenesis. *Biol. Reprod.* 43:543–547.
Channing, C.P., T. Hillensjo, and F.W. Schaerf. 1978. Hormonal control of oocyte meiosis, ovulation and luteinization in mammals. *Clin. Endo. Met.* 7:601–624.
Clifford, R., R. Francis, and T. Schedl. 1994. Somatic control of germ cell development in *Caenorhabditis elegans*. *Semin. Dev. Biol.* 5:21–30.
Collins, J., B. Saari, and P. Anderson. 1987. Activation of a transposable element in the germ line but not the soma of *Caenorhabditis elegans*. *Nature (Lond.)*. 328:726–728.
Davidson, E.H. 1986. Gene Activity in Early Development. Academic Press, New York 670 pp.
Deshaies, R.J., and R. Schekman. 1987. A yeast mutant defective at an early stage in import of secretory protein precursors into the endoplasmic reticulum. *J. Cell Biol.* 105:633–645.
Deshaies, R.J., S.L. Sanders, D.A. Feldheim, and R. Schekman. 1991. Assembly of yeast Sec proteins involved in translocation into the endoplasmic reticulum into a membrane-bound multisubunit complex. *Nature (Lond.)*. 349:806–808.
Diaz-Infante Jr., A., B.S. Wright, and E.E. Wallach. 1975. Influence of estrogen and progesterone treatment on ovarian contractility in the monkey. *Fertil. Steril.* 26:101–110.
Doane, W.W. 1960. Completion of meiosis in uninseminated eggs of *Drosophila melanogaster*. *Science (Wash. DC)*. 132:677–678.
Dobberstein, B. 1994. On the beaten pathway. *Nature (Lond.)*. 367:599–600.
Esnault, Y., M.O. Blondel, R.J. Deshaies, R. Scheckman, and F. Kepes. 1993. The yeast SSS1 gene is essential for secretory protein translocation and encodes a conserved protein of the endoplasmic reticulum. *EMBO (Euro. Mol. Biol. Organ.) J.* 12:4083–4093.
Esnault, Y., D. Feldheim, M.O. Blondel, R. Schekman, and F. Kepes. 1994. SSS1 encodes a stabilizing component of the Sec61 subcomplex of the yeast protein translocation apparatus. *J. Biol. Chem.* 269:27478–27485.
Francis, R., M.K. Barton, J. Kimble, and T. Schedl. 1995. *gld-1*, a tumor suppressor gene required for oocyte development in *Caenorhabditis elegans*. *Genetics*. 139:607–630.
Freeman, M., and D.M. Glover. 1987. The *gnu* mutation of Drosophila causes inappropriate DNA synthesis in unfertilized and fertilized eggs. *Genes & Dev.* 1:924–930.
Freeman, M., C. Nusslein-Volhard, and D.M. Glover. 1986. The dissociation of nuclear and centrosomal division in *gnu*, a mutation causing giant nuclei in *Drosophila*. *Cell.* 46:457–468.
Garriga, G., C. Guenther, and H.R. Horvitz. 1993. Migrations of the *Caenorhabditis elegans* HSNs are regulated by *egl-43*, a gene encoding two zinc finger proteins. *Genes & Dev.* 7:2097–2109.
Görlich, D., and T.A. Rapoport. 1993. Protein translocation into proteoliposomes reconstituted from purified components of the endoplasmic reticulum membrane. *Cell.* 75:615–630.
Görlich, D., S. Prehn, E. Hartmann, K.U. Kalies, and T.A. Rapoport. 1992. A mammalian homolog of SEC61p and SECYp is associated with ribosomes and nascent polypeptides during translocation. *Cell.* 71:489–503.
Greenstein, D., S. Hird, R.A. Plasterk, Y. Adachi, Y. Kohara, B. Wang, M. Finney, and G. Ruvkun. 1994. Targeted mutations in the *C. elegans* POU-homeobox gene *ceh-18* cause defects in oocyte cell cycle arrest, gonad migration, and epidermal differentiation. *Genes & Dev.* 8:1935–1948.
Halloran, N., Z. Du, and R. Wilson. 1991. DNA sequencing: laboratory protocols. *In* Methods in Molecular Biology. Vol. 10. H.G. Griffin and A.M. Griffin, editors. The Humana Press Inc. Clifton, N.J.
Hartmann, E., T. Sommer, S. Prehn, D. Görlich, S. Jentsch, and T.A. Rapoport. 1994. Evolutionary conservation of components of the protein translocation complex. *Nature (Lond.)*. 367:654–657.
Hartwell, L.H., and T.A. Weinert. 1989. Checkpoints: controls that ensure the order of cell cycle events. *Science (Wash. DC)*. 246:629–634.
Hedgecock, E.M., and R.K. Herman. 1995. The *ncl-1* gene and genetic mosaics of *Caenorhabditis elegans*. *Genetics*. 141:989–1006.
Hirsh, D., D. Oppenheim, and M. Klass. 1976. Development of the reproductive system of *Caenorhabditis elegans*. *Dev. Biol.* 49:200–219.
Hodgkin, J., M. Edgley, D. Riddle, and D. Albertson. 1988. Genetics. *In* The Nematode *Caenorhabditis elegans*. W.B. Wood, editor. Cold Spring Harbor Laboratory, Cold Spring Harbor, NY. 491–584.
Horvitz, H.R., S. Brenner, J. Hodgkin, and R.K. Herman. 1979. A uniform genetic nomenclature for the nematode *Caenorhabditis elegans*. *Mol. Gen. Genet.* 175:129–133.
Hunter, C.P., and W.B. Wood. 1992. Evidence from mosaic analysis of the masculinizing gene *her-1* for cell interactions in *C. elegans* sex determination. *Nature (Lond.)*. 355:551–555.
Jones, A.R., and T. Schedl. 1995. Mutations in *gld-1*, a female germ cell-specific tumor suppressor gene in *Caenorhabditis elegans*, affect a conserved domain also found in Src-associated protein Sam68. *Genes & Dev.* 9:1491–1504.
Kanatani, H., H. Shirai, K. Nakanishi, and T. Kurokawa. 1969. Isolation and identification of meiosis inducing substance in starfish *Asterias amurensis*. *Nature (Lond.)*. 221:273–274.
Kimble, J., and S. Ward. 1988. Germline development and fertilization. *In* The Nematode *Caenorhabditis elegans*. W.B. Wood, editor. Cold Spring Harbor Laboratory, Cold Spring Harbor, NY. 191–213.
Kimble, J., L. Edgar, and D. Hirsh. Specification of male development in *Caenorhabditis elegans*: the *fem* genes. *Dev. Biol.* 105:234–239.
Kirby, C., M. Kusch, and K. Kemphues. 1990. Mutations in the *par* genes of *Caenorhabditis elegans* affect cytoplasmic reorganization during the first cell cycle. *Dev. Biol.* 142:203–215.
Kreutzer, M.A., J.P. Richards, M.N. DeSilva-Udawatta, J.A. Knoblich, C.F. Lehner, and K.L. Bennett. 1995. *Caenorhabditis elegans* cyclin A- and B- type genes: a cyclin A multigene family, an ancestral cyclin B3 and differential gemline expression. *J. Cell Sci.* 108:2415–2424.
L'Hernault, S.W., D.C. Shakes, and S. Ward. 1988. Developmental genetics of chromosome I spermatogenesis-defective mutants in the nematode *Caenorhabditis elegans*. *Genetics*. 120:435–452.
Lasko, P.F. 1992. Molecular movements in oocyte patterning and pole cell differentiation. *Bioessays*. 14:507–512.
Li, W., and J.E. Shaw. 1993. A variant Tc4 transposable element in the nematode *C. elegans* could encode a novel protein. *Nucleic Acids Res.* 21:59–67.
Link, C.D., M.A. Silverman, M. Breen, K.E. Watt, and S.A. Dames. 1992. Characterization of *Caenorhabditis elegans* lectin-binding mutants. *Genetics*. 131: 867–881.
Mahowald, A.P., T.J. Goralski, and J.H. Caulton. 1983. *In vitro* activation of *Drosophila* eggs. *Dev. Biol.* 98:437–445.
Maller, J.L., J. Gautier, T.A. Langan, M.J. Lohka, S. Shenoy, D. Shalloway, and P. Nurse. 1989. Maturation-promoting factor and the regulation of the cell cycle. *J. Cell Sci.* 12:53–63.
Masui, Y., and H.J. Clarke. 1979. Oocyte maturation. *Int. Rev. Cytol.* 57:185–282.
Mello, C.C., J.M. Kramer, D. Stinchcomb, and V. Ambros. 1991. Efficient gene transfer in *C. elegans*: extrachromosomal maintenance and integration of transforming sequences. *EMBO (Eur. Mol. Biol. Organ.) J.* 10:3959–3970.
Müsch, A., M. Wiedmann, and T.A. Rapoport. 1992. Yeast Sec proteins interact with polypeptides traversing the endoplasmic reticulum membrane. *Cell.* 69:343–352.
Myers, C.D., P.-Y. Goh, T.S. Allen, E.A. Bucher, and T. Bogaert. 1996. Developmental genetic analysis of troponin T mutations in striated and nonstriated muscle cells of *Caenorhabditis elegans*. *J. Cell Biol.* 132:1061–1077.
O'Farrell, P.H., B.A. Edgar, D. Lakich, and C.F. Lehner. 1989. Directing cell division during development. *Science (Wash. DC)*. 246:635–640.
Panzner, S., L. Dreier, E. Hartmann, S. Kostka, and T.A. Rapoport. 1995. Post-translational protein transport in yeast reconstituted with a purified complex of Sec proteins and Kar2p. *Cell.* 8:561–570.
Patel, N.H., and C.S. Goodman. 1992. Preparation of digoxigenin-labeled single stranded DNA probes for *in situ* hybridization. *In* Non-radioactive Labeling and Detection of Biomolecules. C. Kessler, editor. Springer-Verlag, Berlin. 377–381.
Sanders, S.L., K.M. Whitfield, J.P. Vogel, M.D. Rose, and R.W. Schekman. 1992. Sec61p and BiP directly facilitate polypeptide translocation into the ER. *Cell.* 69:353–365.
Schekman, R. 1994. Translocation gets a push. *Cell.* 78:911–913.
Seydoux, G., and A. Fire. 1994. Soma-germline asymmetry in the distribution of maternal and zygotic mRNAs in early *C. elegans* embryos. *Development (Camb.)*. 120:2823–2834.
Shamanski, F.L., and T.L. Orr-Weaver. 1991. The *Drosophila plutonium* and *pan gu* genes regulate entry into S phase at fertilization. *Cell.* 66:1289–1300.
Shen, M.M., and J. Hodgkin. 1988. *mab-3*, a gene required for sex-specific yolk protein expression and a male-specific lineage in *C. elegans*. *Cell.* 54:1019–1031.
Stirling, C.J., J.J. Rothblatt, M.M. Hosobuchi, R.R. Deshaies, and R.R. Schekman. 1992. Protein translocation mutants defective in the insertion of integral membrane proteins into the endoplasmic reticulum. *Mol. Biol. Cell.* 129–142.
Strome, S. 1986. Establishment of asymmetry in early *Caenorhabditis elegans* embryos: visualization with antibodies to germ cell components. *In* Gametogenesis and the Early Embryo. J.G. Gall, editor. Alan R. Liss Inc., New York. 77–95.
Sulston, J., and J. Hodgkin. 1988. Methods. *In* The Nematode *Caenorhabditis elegans*. W.B. Wood, editor. Cold Spring Harbor Laboratory, Cold Spring Harbor, NY. 587–606.
Sulston, J.E., and H.R. Horvitz. 1977. Post-embryonic cell lineages of the nematode *Caenorhabditis elegans*. *Dev. Biol.* 56:110–156.
Sulston, J.E., and J.G. White. 1980. Regulation and cell autonomy during postembryonic development of *Caenorhabditis elegans*. *Dev. Biol.* 78:577–597.
Sulston, J.E., E. Schierenberg, J.G. White, and J.N. Thomson. 1983. The embryonic cell lineage of the nematode *Caenorhabditis elegans*. *Dev. Biol.* 100:64–119.
Ward, S., and J.S. Carrel. 1979. Fertilization and sperm competition in the nematode *Caenorhabditis elegans*. *Dev. Biol.* 73:304–321.
Ward, S., and J. Miwa. 1978. Characterization of temperature-sensitive, fertilization-defective mutants of the nematode *Caenorhabditis elegans*. *Genetics*. 88:285–303.
Wharton, D.A. 1983. The production and functional morphology of helminth egg-shells. *Parasitology*. 86:85–97.
White, J.G., E. Southgate, J.N. Thomson, and S. Brenner. 1986. The structure of the nervous system of *Caenorhabditis elegans*. *Philos. Trans. R. Soc. Lond. B Biol. Sci.* 314:1–340.
Wickramasinghe, D., and D.F. Albertini. 1993. Cell cycle control during mammalian oogenesis. *Curr. Top. Dev. Biol.* 28:125–153.
Yuan, J.Y., M. Finney, N. Tsung, and H.R. Horvitz. 1991. Tc4, a *Caenorhabditis elegans* transposable element with an unusual fold-back structure. *Proc. Natl. Acad. Sci. USA*. 88:3334–3338.